Tying skin deformation patterns with discriminability of compliance to design soft haptic actuators

A

Dissertation

Presented to

the faculty of the School of Engineering and Applied Science

University of Virginia

in partial fulfillment

of the requirements for the degree

Doctor of Philosophy

by

Bingxu Li

May 2023

APPROVAL SHEET

This

Dissertation

is submitted in partial fulfillment of the requirements
for the degree of

Doctor of Philosophy

Author: Bingxu Li

Advisor: Gregory Gerling

Advisor:

Committee Member: Sara Riggs

Committee Member: Seongkook Heo

Committee Member: Tariq Iqbal

Committee Member: Miguel Otaduy

Committee Member:

Committee Member:

Accepted for the School of Engineering and Applied Science:

Jennifer L. West, School of Engineering and Applied Science

May 2023

Abstract

Of the various dimensions that underlie our sense of touch – e.g., roughness, texture, and stickiness – compliance is particularly important in our daily lives. For example, we routinely inspect the ripeness of fruit and affectively touch others. To discriminate the compliance of soft and compliant objects, we rely upon spatiotemporal cues in the mechanical deformation of the skin, which is embedded with hundreds of neural afferents. However, since direct observations of skin dynamics are challenging, we do not yet understand, in touching objects of various compliance, how skin deformation patterns evolve over time and thereby inform perceptual judgements, how do such relations vary among individuals, and how can we create a close-loop system that simulates tactile sensations with simultaneous observation of skin dynamics. First, to obtain visual access of skin dynamics and quantify skin deformation, we developed a 3-D stereo imaging technique for use in passive touch to observe contact of the skin's surface with transparent, compliant substrates. In doing so, we derive skin deformation cues to quantify and characterize the skin's movements with varying stimulus compliance, indentation depth, velocity, and time duration. Our results indicate that compliant stimuli at higher velocities are more difficult to discriminate because they induce smaller differences in deformation, beyond a minimum contact duration of 0.4 seconds. Moreover, we find that several independent cues aid our perception of compliance. In particular, the change rate of contact area best correlates with tactile discriminability regardless of indentation velocities and stimulus compliance, while cues associated with skin curvature and bulk force are predictive for stimuli more and less compliant than skin, respectively. Second, we study the differences in skin properties and tactile acuity among individuals where factors of skin stiffness and fingerprint breadth have been underexplored. Therefore, we recruited a cohort of young participants who present a diverse range of finger size, stiffness, and fingerprint breadth, and investigated relationships between their fingertip properties and perceptual discriminability. We found that the ability of participants to discriminate compliance could be differentiated by their finger stiffness. In support of this finding, in softening the participants' skin with hyaluronic acid, we observed an improvement in their perceptual discriminability, which further validates the high correlation between finger stiffness and perception. Finally, to develop a close-loop haptic

system, we designed a transparent, reconfigurable, multi-channel hydraulic haptic actuator. Through actuation, we can control the movement of skin surface and optically observe skin deformation with distinct elasticities that produce distinct percepts. Profiles of the contacting surface are directly visualized through actuated channels to match observations with solid substrates, and seek to enable personalized calibration in the future.

Acknowledgments

This work was supported in part by the National Science Foundations (IIS-1908115, NRT-1829004) and National Institutes of Health (NINDS R01NS105241). The funders had no role in study design, data collection and analysis, decision to publish, or preparation of the manuscript.

I would like to thank Professor Gregory Gerling for his many years of mentorship and support.

I reserve a final note for my family. I thank my parents and my brother for their unconditional love and support. I thank my husband who gave me tremendous help and always stood by my side throughout this journey. I would also like to thank to my dog, Meimei, who brought me consistent joy and comfort.

Table of Contents

ABSTRACT 1

ACKNOWLEDGMENTS 3

OVERVIEW OF AIMS 7

BACKGROUND 10

AIM 1: CHARACTERIZE CHANGE OF SKIN DEFORMATION EVOKED UPON INDENTATION IN VARYING STIMULUS COMPLIANCE, VELOCITIES, DEPTHS AND CONTACT DURATIONS 13

INTRODUCTION 13

MATERIAL AND METHODS 14

Apparatus 15

Compliant stimuli fabrication 15

3-D surface reconstruction and image processing 16

Ellipse method to generate image planes 17

Derived dependent metrics 17

Human-subjects experimental paradigm 18

Participants 18

Psychophysical experiments 18

Biomechanical experiments 19

Statistical analysis 19

RESULTS 21

Results of Psychophysical experiments 21

Approach 1: skin deformation at discrete time points 21

Approach 2: change rate of skin deformation over the time course of the indentation 22

Dependency between skin deformations cues 24

DISCUSSION 28

Indentation duration and velocity shape discrimination 29

The utility of distinct skin deformation cues 30

Discrimination strategies for rate-based encoding 31

AIM 2: EVALUATE THE IMPACT OF INDIVIDUALS' SKIN PROPERTIES ON THEIR TACTILE DISCRIMINABILITY **32**

INTRODUCTION 32

MATERIAL AND METHODS 34

Participants *34*

Stimulus fabrication *34*

Measurements of finger skin properties *35*

Psychophysical experiments *36*

Biomechanical experiments *36*

Skin stiffness modulation *37*

Statistical analysis *37*

RESULTS 37

Experiment 1: Relationships between finger properties and perceptual discrimination *38*

Experiment 2: Characterization of skin surface deformation *39*

Experiment 3: Individual differences in finger properties modulate skin deformation and perceptual discrimination *40*

Experiment 4: Decoupling the impact of fingertip size and skin stiffness on perceptual discrimination in subgroups of participants *41*

Experiment 5: Decreasing skin stiffness improves one's perceptual discrimination *42*

DISCUSSION 50

Importance of finger stiffness in predicting individual discrimination performance *50*

Two distinct participant groups (can be used to approximate) that predict discrimination performance *51*

Skin deformation cues useful as a surrogate for neural population response *52*

Changing skin mechanics state influences perception *53*

AIM 3: DESIGN SOFT HAPTIC ACTUATORS TO VISUALIZE THE FINGER PAD SURFACE AT DISTINCT PERCEPTS OF COMPLIANCE **53**

INTRODUCTION 53

MATERIAL AND METHODS 55

Fabrication of transparent, multi-channel actuator *55*

Validation of actuator mechanics and transparency *56*

Validation of actuator with human-subjects *57*

RESULTS 58

Results of actuator mechanical performance *58*

Results of actuator imaging transparency *59*

Results of biomechanical human-subjects experiments *59*

Results of psychophysical human-subjects experiments *60*

DISCUSSION 63

OVERALL CONCLUSIONS AND FUTURE WORK 65

PUBLICATIONS 67

REFERENCE 69

Overview of aims

Our sense of touch is a powerful tool that helps us effectively communicate and interact with others and our environment. In contacting a surface, we are able to acquire information about an object's physical properties such as its softness, texture and shape; and we can naturally convey social expressions such as excitement and happiness with other people. Our skin is a deformable and stretchable organ that enables and encodes mechanical contact through hundreds of neural afferents that are embedded within. Those afferents are extremely sensitive to external stimuli and are recruited by subtle deformation at the skin surface. We rely on their input to interpret the physical properties of an object, in which compliance is a prominent attribute amongst others, due to its importance in our daily activities especially with natural objects. To encode the compliance of an object, we utilize spatial and temporal cues generated in deformation of the skin which then are further transited to our brain for making perceptual judgements. Therefore, it is important to understand how those cues evolve over the course of time and how they drive our percepts.

The overall objective of this dissertation is to address the correlation between skin deformation and tactile perception of material compliance. We investigate factors of indentation velocity, depths, contact time duration, stimulus compliance, and evaluate their impact on perceptual discriminability of compliance. We further study differences in skin properties including finger size, stiffness, and ridge breadth across individuals, and how those factors affect perceptual acuity. We employ 3-D imaging techniques to optically observe skin movements which are characterized as skin cues, and we conduct human-subject experiments in psychophysical evaluations. The correlation between physical contact and perceptual responses is evaluated by regression analysis, and using such correlation statistical models are built to predict individuals' discrimination performance. Ultimately, we design and fabricate a soft haptic actuator that modulates skin movements to drive distinct percepts while maintaining direct visualization of contact surface during actuation.

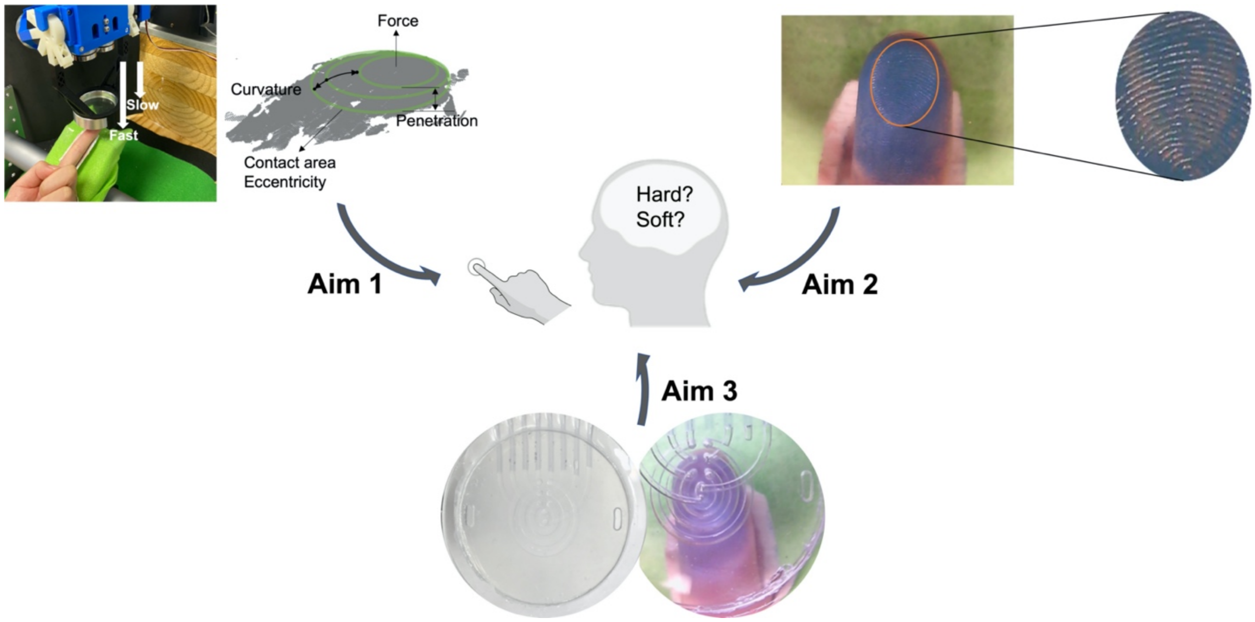

Figure 1.1. Scope of this dissertation. Aim 1 characterizes the change of skin deformation evoked upon indentation by objects varying in compliance, velocity, depth and time duration. Aim 2 evaluates the impact of fingertip properties on one's discrimination performance. Aim 3 designs a soft haptic actuator that produces distinct and naturalistic percepts of compliance.

Aim 1: Characterize change of skin deformation evoked upon indentation in varying stimulus compliance, velocities, depths, and contact durations. To help in discriminating compliance of an object, we rely upon cues within the spatial and temporal deformation of the skin. To empirically understand how such cues evolve over the course of stimulus indentation, and drive perceptual response, we developed a 3-D stereo imaging technique to observe the skin through transparent, compliant stimuli. Passive-touch experiments were conducted with stimuli varying in compliance, as well as indentation velocity, depth and contact time duration. Image processing methods were employed to pre-process images for noise reduction and for selecting regions of interests. Then we developed spatiotemporal cues to characterize skin deformation by using geometric modeling. In experiments with human participants, factors considered including differentiating between objects softer and harder than skin, and determining how indentation velocities influence the evolution of cues and percepts, in space and time. Finally, we tied skin deformation with psychophysical responses in discrimination tasks to decipher our percepts in compliance.

Aim 2: Evaluate the impact of individuals' skin properties on their tactile discriminability. Individual differences in tactile acuity are observed within and between age cohorts, which may result from many factors including gender, age, finger size and stiffness, as well as additional cognitive and behavioral factors. This aim considered individual differences, within a younger cohort of participants, in discriminating compliant surfaces with a focus on finger stiffness, size and fingerprint ridge breath which were measured by a digital caliper, rigid body compression test and image processing tools, respectively. Next, the participants completed pairwise psychophysical discrimination of sets of compliant surfaces, ranging from stiffer to softer than finger pad skin. Along with the psychophysical evaluation, we used machine learning models to find distinct groups with differences in skin properties and perceptual performance. Then, we built statistical models to predict an individual's tactile discriminability based on the skin properties. Finally, to further validate the results from those models we directly modulated the skin state and the changes in perception were observed.

Aim 3: Design soft haptic actuators to visualize the finger pad surface at distinct percepts of compliance. The virtual rendering of compliance, or 'softness', at the finger pad may enable interactions such as touching the hand of another or of tissue in surgery. Though numerous tactile interfaces have shown programmable compliance, most are evaluated only perceptually. In contrast to those, this aim sought to demonstrate control of the deformation of the skin surface, by optically observing it being indented with elasticities that product distinct percepts. First, we evaluated the mechanical parameters of the actuator including vertical displacement, inner channel pressure and contact force. Second, the 3-D imaging method was used to generate skin profiles of contact surface at various actuation states, and those profiles were then compared with solid substrates. Ultimately, psychophysical experiments were conducted to validate the actuator's performance in delivering differentiable percepts of compliance.

Background

Rendering technologies for skin cues that underlies percept of compliance. Our percept of compliance is thought to be encoded by cues at various points in the body, notably at the skin contact interface, though as well at joints and muscles, skin regions on the back of the digits and hand, and near the nail [1]–[3]. The utility of particular cues may be tied to the magnitude of compliance of the stimulus, and the relevant cues are likely involve contact area [4], [5], penetration depth [6], contact force [7], [8], skin stretch and surface stress [9]. For example, in prior work, Srinivasan and LaMotte noted that compliances near the modulus of skin tissue or less may be perceived differently than those stiffer [10]. Likewise, subsequent work shows that force-related cues are optimal for the range stiffer (~160 kPa) but not softer (~30 kPa) [11].

To identify cues that evoke a percept of compliance, we need to understand how the skin's surface deforms in space and time, while in contact with an object. Along these lines, empirical measurements and unique experimental paradigms were developed to study skin deformation cues that associate with our perceptual responses. For instance, elastomeric slabs have been fabricated at controlled thickness and distances to consider the effects of indentation depth and contact area on tactile perception [6]. Ink-based methods have estimated contact area at the terminal point of indentation [11], [12]. More recently, vision-based approaches have provided high resolution empirical measurements of the contact surface using cameras in order to observe time-dependent changes in the skin. Usually, rigid surfaces such as glass plates are brought to the finger and a camera captures the image of skin surface for evaluation. This technique has been employed for slip detection and friction rendering [13]–[15].

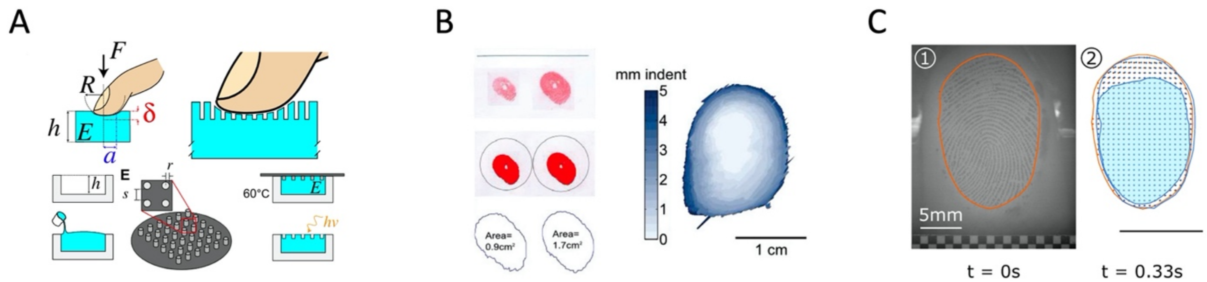

(Dhong et al., 2019) *(Hauser and Gerling, 2018)* *(Barrea et al., 2018)*

Figure 1.1. Prior experimental paradigms to examine skin deformation cues. (A) Elastomeric slabs for contact area and penetration depth. (B) Ink-based method for contact area at terminal indentation. (C) Camera-based technique for contact area.

Individual differences in skin mechanics and tactile acuity. As haptic displays become ubiquitous, designers are beginning to adapt them to individual users. To effectively do so, we need to understand the extent and impact of individual differences, which can impact the efficacy of such displays [16]. Indeed, individual differences in tactile acuity are observed within and between age cohorts. Prior scientific investigations indicate that such differences may result from many factors, including skin properties such as finger size and stiffness, sex/gender, age, as well as additional developmental, cognitive, and behavior aspects. In particular, those with smaller fingers exhibit better tactile spatial acuity [17], [18]. The rationale is that smaller fingers, with the same number of tactile afferents, afford a higher density to inform our perceptual judgements. Age and gender, in addition, may influence tactile performance. For instance, 2-point discrimination thresholds increase for elderly as compared to young cohorts [19]. As one contributing factor, decreased tactile acuity is expected as we age due to a loss of elastin fibers and with it increased wrinkling of the skin. Finger pad skin stiffness – decoupled from aging – may impact tactile acuity, as the work of Vega-Bermudez and Johnson indicates, though there is not yet consensus on this topic. In particular, Woodward and Peters found no relationship between skin compliance and tactile acuity [18], [20], however, Vega-Bermudez and Johnson argued that that such results could be biased due to the compliance calculation, group division for the statistical tests, and the variance of acuity measurements [21]. This work indicated that young people with softer fingers have lower tactile detection thresholds, which aligns with finite element analysis of the skin [22].

Design approaches of haptic actuator that render compliance. The emergence of haptic interactions embedded into wide-ranging applications - in virtual reality, medical simulation, surgical training, and soft robotics - demands human-computer interfaces (HCI) with reconfigurable, natural, and portable feedback. To effectively create dynamic haptic sensations with soft objects, displays involving various actuation approaches have been explored. The most common approaches utilize hydraulic [23], [24] and pneumatic mechanisms [25], [26], which use fluids or gases to deform the geometry of the contact surface. More recently, non-contact actuation techniques involving air flow and ultrasound have been proposed [27], [28]. Another approach is to use magnetism so that the mechanical properties of fillers respond to an externally applied field, such as with magnetorheological (MR) fluids [29]. Skin-like, soft and conformable interfaces are appealing in the field of HCI because they provide users with more comfortable and natural touch interactions than traditional rigid interfaces. For instance, prior works with soft user interfaces have explored printing soft dielectric materials or conductive ink on elastomers [iSkin, Tacttoo, Tactile Widget, Aditya and Daniel's work, skin-on interfaces].

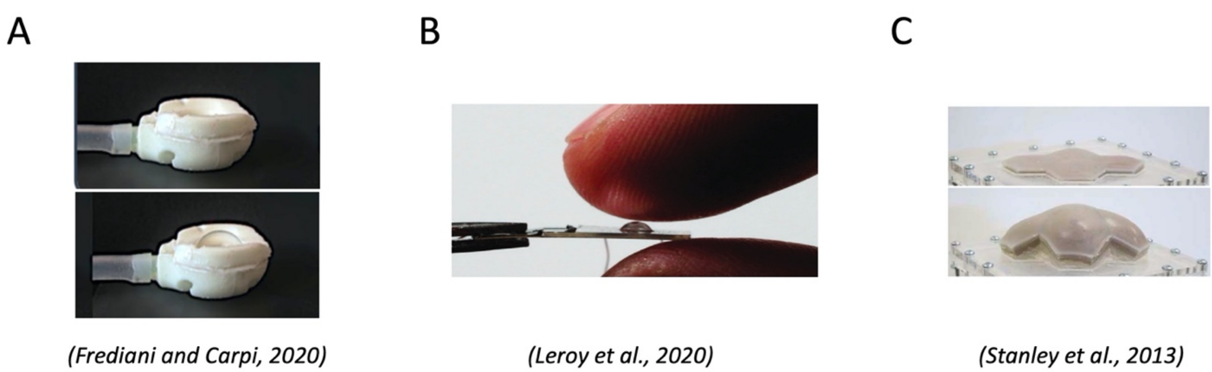

Figure 1.2. Actuation approaches that have been commonly used for delivering compliance sensations. (A) Pneumatic actuation. (B) Hydraulic actuation. (C) Jamming technique using sparse particles.

Aim 1: Characterize change of skin deformation evoked upon indentation in varying stimulus compliance, velocities, depths and contact durations

Introduction

The skin is a deformable and stretchable organ embedded with thousands of neural afferents that encode mechanical contact interactions. Observations of its surface over time are vital to deciphering how we perceive the physical properties of objects, such as softness, roughness, and texture, amongst others. Within the broad category of softness [30], an object's compliance is important in our daily activities, e.g., inspecting the ripeness of fruit [31]. Understanding both how compliant stimuli are encoded at the skin's surface and how such deformation patterns evoke a percept is a fundamental topic and prerequisite in designing haptic actuators [23], [32], [33] and rendering algorithms [34]. Our percept of compliance is thought to be encoded, most notably, in cutaneous skin tissue near the contact interface [5], [35], [36], though also at joints and muscles [2], [37], non-contacting skin regions on the back of the digits and hand [3], and near the nail [38]. Moreover, as Xu, et al. show in modulating cutaneous inputs, our percept of compliance is a product of both sensation and volition [37]. At the skin contact interface, the relevant mechanical cues are not yet resolved, but likely involve gross contact area [4], [5], indentation depth [6], contact force [7], [8], skin stretch [6], [8], and surface stress [9]. Also, likely vital is their evolution over the time-course of contact [11], [35], [39].

To evaluate relationships of these mechanical cues with perception, a variety of empirical measurement techniques and experimental paradigms have been employed. For instance, in fabricating elastomeric slabs with controlled thickness and surface structure, Dhong et. al found that indentation depth and contact area contribute independently to perceived compliance [6]. Ink-based methods have estimated contact area at an indentation's terminal point [9], [11]. Similarly, stationary foam displays with a joint angle encoder have evaluated the contributions of finger displacement, joint angle, and change in contact area [5]. Spring cells with rigid plates have explored relationships of force and displacement, finding kinesthetic input alone is insufficient to discriminate compliance [10]. Similarly, Bergman, Tiest and Kappers used elastomeric cylinders to compare kinesthetic force and displacement with cutaneous skin surface deformation cues, showing the importance of the latter [36], [40]. Moreover, sensors using piezoelectric materials at the skin surface have been built to assess contact area spread rate, pressure distribution, stress rate, slip detection, and force feedback [4], [41]–[43], while mechatronic devices have considered surface stretch [44], [45].

However, prior works have not directly observed the time-course of the skin surface while in contact with compliant objects, nor captured the how its deformation response differs with indentation velocity, depth, and duration, thereby shaping our perceptual judgments. Considering such factors are necessary given the skin's non-linear and time-dependent properties [46]. Moreover, prior studies indicate indentation velocity can influence neural firing and our perception of compliance [47]–[49]. Therefore, in effort to tease apart the mechanical cues at the skin surface that most optimally drive our perceptual response, across a range of stimuli varying in compliance, indentation depth, velocity, and time duration, the work herein develops equipment and an experimental approach to image the time-course of the skin surface while in contact with transparent, compliant stimuli.

Material and Methods

To measure how spatiotemporal cues evolve over the course of contacting soft, compliant objects, we developed a 3-D stereo imaging method. Silicone-elastomer stimuli were fabricated that span a range of compliances greater and lesser than that of the finger pad skin. From images of the skin surface taken through transparent stimuli, 3-D point clouds that represent the geometry of the surface deformation of the finger pad are generated every 100 ms using a disparity-mapping algorithm. These measurements were distilled into skin deformation cues of contact area, penetration depth, eccentricity, curvature, and force; and their time derivatives. Psychophysical experiments of pairwise discrimination, using a two-alternative forced choice (2AFC) strategy, in passive touch, were conducted across a prescribed range of stimulus compliances (5 to 184 kPa), as well as indentation depths (1.0 and 2.0 mm), velocities (1.0 to 6.5 mm/s), and time durations (0.3 to 2.0 s).

In particular, the experimental paradigm included discrimination of stimuli less than skin, more compliant than skin, and overlapping with the skin's compliance. As well, it includes three cases where the time duration was equalized by varying velocity and indentation depth (e.g., 2.5 mm/s at 1 mm and 4.5 mm/s at 2 mm, where both yield a time duration of 0.4 s).

Apparatus

An abbreviated description of the imaging apparatus is provided below and in Fig. 2.1A. For additional details on its validation, refer to prior work [50], [51]. Overall, the apparatus consists of an electrical-mechanical motion controller and load sled (ILS-100 MVTP, Newport, Irvine, CA, USA) with two cameras and a load cell installed on a cantilever. Up to five compliant stimuli can be delivered individually to a stationary finger pad at controlled indentation depth, velocity, and duration. Participants are seated in an adjustable chair with their elbow resting on a table surface during an experiment. Each participant's forearm is placed on a custom rigid support, oriented at an angle of 30 degrees with respect to the table's horizontal surface. A plastic curved support fixes the finger position beneath the point of contact. An aluminum disk with a glass plate on the non-contact side houses each silicone-elastomer stimulus. Several stimuli were fabricated that vary in modulus and were mounted within custom 3D printed plastic arms to a rotary center, controlled by a servo motor. Displacement of a stimulus into the finger pad surface is controlled and measured by the motion controller, and force is measured at the stimulus by a load cell at 150 Hz, with a resolution of ±0.05 N (LCFD-5, Omegadyne, Sunbury, OH, USA). Two webcams (Papalook PA150, Shenzhen Aoni Electronic Industry Co., Guangdong, China) above the stimulus capture images at 30 frames per second, at a maximum resolution of 1280 by 720 pixels, and are able to maintain a manual focus.

Compliant stimuli fabrication

Seven silicone-elastomer stimuli were constructed with modulus values from 5 to 184 kPa. For reference, the bulk modulus of human skin at the finger pad is about 42 – 54 kPa [52], [53]. One stimulus (45 kPa) lies within this range, with three stimuli fabricated to be more compliant (5, 10, 33 kPa) and three less compliant (75, 121, 184 kPa). Each formulation of silicone-elastomer was poured into its container, made by sealing a clean, dry glass disc (5.1 cm radius by 0.3 cm thick) into an aluminum collar (5.4 cm outer radius by 1.6 cm thick) using 0% diluted Solaris and heated at 100 Celsius until fully sealed. The more compliant stimuli (5, 10, 33 kPa) were made of two-component silicone rubber (Solaris, Smooth-on Inc., Macungie, PA, USA), mixed at a 1:1 ratio and then diluted with silicone oil (ALPA-OIL-50, Silicone oil V50, Modulor, Berlin, Germany) at ratios of 400% (4:1 ratios of silicone rubber to oil) for 5 kPa, 300% for 10 kPa and 200% for 33 kPa. Each stimulus rested at room temperature until its air bubbles were released, then cured in an oven at 100° Celsius for 25 min to fully solidify, before being returned to room temperature. To eliminate surface stickiness, a 0.04 mm layer of 100% diluted Solaris silicone rubber was applied to each substrate's surface, before being cured at 100° Celsius for 15 min. Stimuli harder than skin (75, 121, 184 kPa) were made of a different two-component silicone rubber (Sylgard 184, Dow Corning, Midland, MI, USA), mixed with silicone oil at ratios of 100%, 50%, and 0% respectively. A sample (0.1 cm diameter by 0.1 cm height) was extracted for measuring the modulus of each stimulus formulation, indented by a glass plate at 1 mm/s velocity and 1 mm depth. The modulus of the stress-strain curve obtained from the force-displacement data was evaluated at 0.1 strain, following a standardized procedure [53].

3-D surface reconstruction and image processing

To generate 3D point cloud data that captures the surface deformation of finger pad skin, a disparity-mapping based approach was used, as defined previously [50], [51]. Point clouds were obtained by co-locating the ink points on the skin surface. The identified pixel brightness values between left and right images are the coordinates of the points in the 3D domain (Fig. 2.1B). For noise reduction, we first filtered out high-frequency noise caused by surrounding light sources, then manually extracted the area of contact between the skin and stimulus by masking the remaining areas (Fig. 2.1C). On average, each 3D point cloud contains about 30,000 discrete points after noise reduction. We apply these two steps (filtering and masking) per image frame to ensure the data lie within the region of interest (Fig 2.1D).

Ellipse method to generate image planes

To characterize the geometric change of the skin surface over the time-course of indentation, we developed a method to fit the 3D point cloud into vertically stacked ellipses with the same orientation [51]. The benefits of this ellipse representation are in its dimensionality reduction and data denoising, from 30,000 discrete points. We defined each ellipse as an image plane. Each ellipse contains at least 98% of the points in an image plane with 95% confidence. With the procedure, the 3-D point cloud is divided into image planes at an increment of 0.25 mm, which is twice the resolution of the stereo images in the vertical dimension, i.e., 0.12 mm [50], starting from the plane representing surface contact through that with deepest finger pad penetration. Therefore, the first image plane was defined as the ellipse with deepest finger pad penetration and the last image plane represents the contact surface (Fig. 2.1E, F).

Derived dependent metrics

From using the ellipse method to characterize the geometric change of the skin surface, five dependent metrics, or skin deformation cues, were defined as penetration depth, curvature, eccentricity, contact area, and force.

Penetration depth is defined as the distance between the first and last image plane, in units mm, Eqn. (1), where N is number of image planes. *Curvature* is defined by discrete slope values averaged across all ellipses for that point cloud, Eqn. (2). The slope between two adjacent ellipses is estimated by the radius of the major axis of the ellipse and distance between them, with r as the radius and i the image plane.

$$P = (N - 1) * 0.25 \qquad (1)$$

$$Slope_{ave} = \frac{\sum_{i=1}^{i=N} \frac{r(i+1) - r(i)}{r(i)}}{r(i)} \qquad (2)$$

$$e = \sqrt{1 - \frac{b^2}{a^2}} \tag{3}$$

Eccentricity is used to describe the shape of the contact surface, Eqn. (3), where *a* is the semi-major axis and *b* is the semi-minor axis of the defined ellipse. Eccentricity equals 0 if the contact shape is a perfect circle. contact area, represents the last formed ellipse, at the surface contact plane which is always the largest ellipse. Force is measured from the load cell. This method of estimating contact area has been validated previously [50], [54]. Those skin deformation cues would be applied in Aim 2 and Aim 3 as well.

Human-subjects experimental paradigm

Biomechanical measurements of skin surface deformation and psychophysical experiments of pairwise discrimination were conducted, in passive touch. The seven stimulus compliances (5, 10, 33, 45, 75, 121, and 184 kPa were delivered to the center of the finger pad individually, using displacement-control, at velocities of 1, 1.75, 2.5, 3.5, 4.5 and 6.5 mm/s to depths of both 1 and 2 mm, without any hold of the stimulus after the end of the ramp. The time duration of the loading phase ranged from 0.3 s (3.5 mm/s at 1 mm) to 2 s (1 mm/s at 2 mm).

Participants

A total of 10 participants (mean = 23, SD = 1.2, 6 male and 4 female) were enrolled in the experiments, which all fully completed. The experiments were approved by the local Institutional Review Board, and informed consent was obtained from each participant. All devices and surfaces were sanitized after each use, and participants wore facemasks, according to SARS-COVID-2 protocols. During the perceptual experiments, participants were blindfolded to eliminate any visual cues.

Psychophysical experiments

A series of psychophysical experiments of pairwise discrimination were performed to evaluate combinations of stimulus compliance, across indentation velocity, depth and duration. Four compliant pairs (184/121, 33/5, 45/10, and 45/75 kPa) were used, whereby the 184/121 kPa pair is less compliant than the skin, and the 33/5 kPa is more compliant than the skin, and the remaining pairs span the skin's modulus in either direction. Each stimulus of a pair of stimuli was delivered to a participant's finger pad sequentially in randomized order with a 2 s interval. Participants reported which of the two stimuli was more compliant, either first or second. In total, there were 4,800 indentations, consisting of 2 stimuli within a pair, 4 compliant pairs, 6 velocities, 2 depths, 5 repetitions, and 10 participants. The average experimental duration per participant was about 80 min including breaks. The biomechanical and psychophysical experiments could have been conducted all in one, but we separated them to attain the highest quality imaging data. Such can involve cleaning a small amount of residue from the transparent stimuli, which requires time per indentation (3-5 s) and can produce a lengthier, inconsistent duration between paired psychophysical experiments. Furthermore, each participant's psychophysical experiment was conducted before their biomechanical experiment, as it required greater cognitive attention.

Biomechanical experiments

A series of biomechanical experiments of skin surface deformation evaluated these same stimulus combinations. In total, we analyzed 2,520 indentations, including 7 stimulus compliances, 6 velocities, 2 depths, 3 repetitions, and 10 participants. Note that at the indentation depth of 1 mm, since the compliant pairs were not discriminable at 3.5 mm/s, we did not examine velocities any faster. The average time to complete this experiment was 70 min, including a 10 min break. At the beginning of each participant's experiment, their index finger was secured to a curved plastic support and a thin layer of blue ink was applied using a paint brush, with its bristles normal to the skin surface. Each stimulus was brought into the finger pad with a light contact force (< 0.1 N) before indentation, then slowly retracted to 0 N. This pre-calibration procedure helped ensure a consistent contact state between trials.

Statistical analysis

All image processing procedures were performed using MATLAB Computer Vision Toolbox and all data analysis were performed using Python 3.6. ANOVA tests evaluated statistical differences at $p < 0.05$.

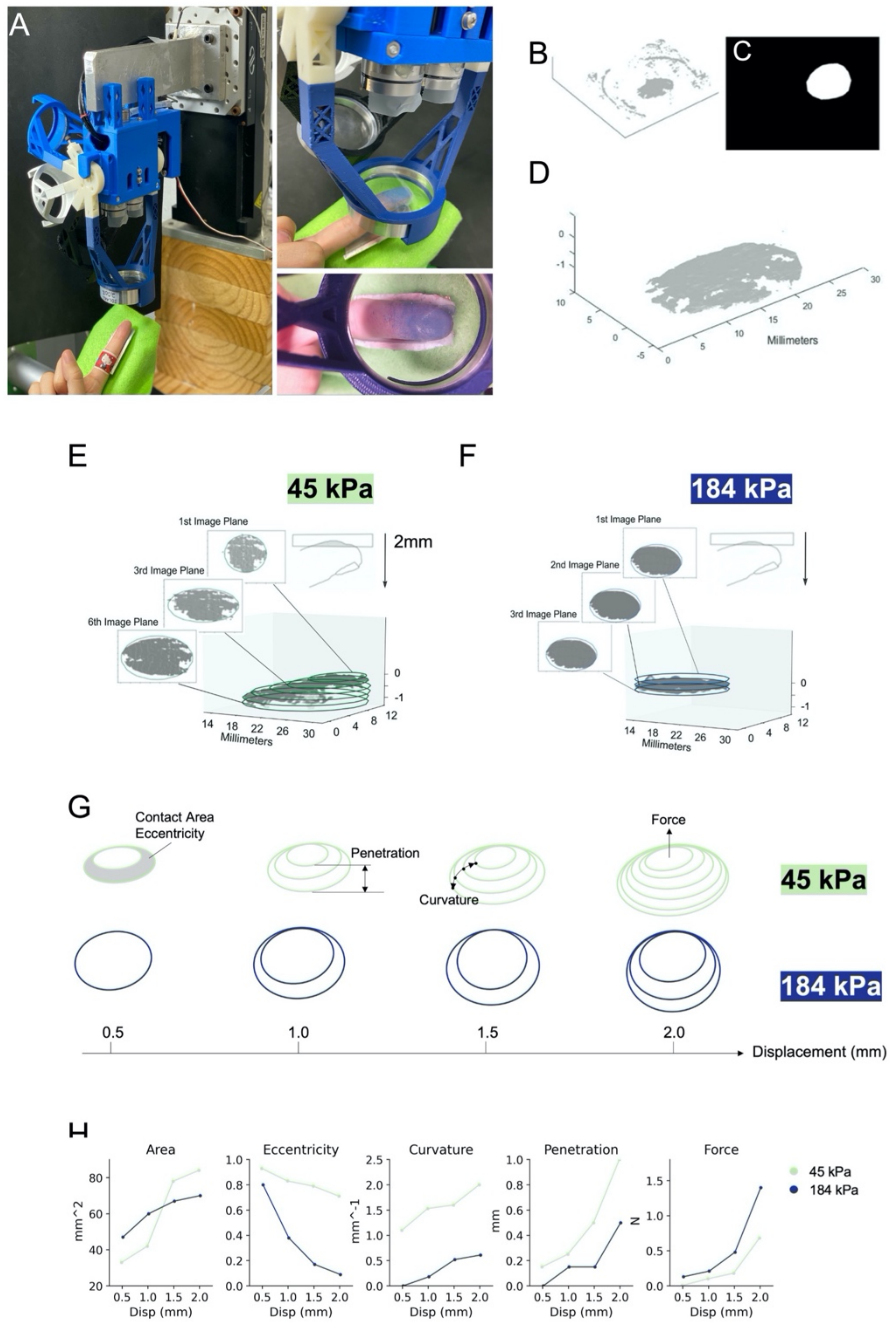

Figure 2.1. Mechanical indentation and imaging apparatus, and data processing procedures, to capture 3D point clouds representing skin surface deformation upon indentation with compliant stimuli. (A) Apparatus with cantilever, 3D printed fixtures, cameras, load cell, and stimuli, relative to the indentation of a participant's finger. A 184 kPa stimulus in contact (left camera image) with a participant's finger pad at an indentation depth of 2 mm. **(B-D)** Data processing of a 3D point cloud, with raw data of the finger pad and partial outline of the aluminum ring at the surface image plane, masking of peripheral noise in the point cloud, and refined point cloud post-masking. **(E-F)** Ellipses are fit to each point cloud at image planes in 0.25 mm increments for more compliant (45 kPa) and less compliant (184 kPa) stimuli at a terminal indentation depth of 2 mm. **(G)** The evolution of the ellipses over the time course of a 2 mm indentation as the finger pad contacts stimuli of two compliances, along with a graphical description of the derived skin deformation cues. **(H)** The comparison of the time course evolution of five skin deformation cues between the two stimuli. One can observe, for instance, that the contact area is larger for the more compliant stimulus (45 kPa) and grows more slowly, while the force is higher for the less compliant stimulus (184 kPa).

Results

Results of Psychophysical experiments

Fig. 2.2A illustrates the modulus of the four compliant pairs, relative to the bulk modulus of the skin. Fig. 2.2B-C show the results in discriminating stimuli at 1 and 2 mm indentation depths, across indentation velocities. Overall, no participant was able to discriminate a stimulus pair at a time duration of less than 0.4 s. In particular, the 45/10 kPa compliant pair was discriminable above 75% correct at indentation velocities of 2.5 and 4.5 mm/s, and slower, at depths of 1 and 2 mm, respectively. Moreover, as Fig. 2.2B-C indicate, participants were less able to correctly discriminate compliant pairs at lower displacements and higher velocities. The 45/10 kPa pair was the most discriminable, and nearly so at a velocity of 6.5 mm/s at 2 mm. In contrast, the 75/45 kPa compliance pair was never reached a 75% level of correct discrimination. The discrimination rates for the 184/121 and 33/5 kPa pairs were higher than the 75% discrimination threshold, where the compliance values of these pairs lie to either side of the skin's modulus.

Furthermore, we performed a 3-way repeated ANOVA test of the major experimental factors, yielding significant effects for compliant pair ($F_{3,387}$ =565.7, p<0.001), velocity ($F_{5,387}$ =1427.8, p<0.0001) and depth ($F_{1,387}$ =1072.5, p<0.0001).

Approach 1: skin deformation at discrete time points

In a first approach to comparing the skin deformation cues and perceptual judgments, we evaluated the cues at discrete observation time points, every 0.1 s. In particular, we conducted pairwise statistical t-tests between compliant pairs every 0.1 s from 0.1 s to the terminal duration of that indentation. Data for the eccentricity cue are shown in Fig. 2.3, with that for all cues in Appendix, Fig. A1 and Fig. A2. As can be observed in Fig. 2.3A, at a stimulus depth of 1 mm and velocity of 1.75 mm/s, there are 6 observation points for each of the 7 compliant stimuli, where eccentricity decreases with indentation time. In Fig. 2.3B, the 0.6 s time point alone is analyzed, as highlighted with the grey bar in Fig. 2.3A. Statistical evaluations of four compliant pairs are given in Fig. 2.3C, where a colored tile indicates statistical significance (p<0.05), and the framework's background of white (1 mm depths) or grey (2 mm depths) indicates a lack of statistical significance.

These four pairs are all statistically significant. Note in Fig. 2.3C the red frames around a group of four tiles, which refers to an evaluation of perceptual discriminability at or above 75% correct, with a diagonal within these tiles indicating a lack of perceptual discriminability. These data come from Fig. 2.2. In this way, one can compare differences in skin deformation cues and perceptual judgments. At least two observations can be made in Fig. 2.3. First, for some of the cues, notably eccentricity, we observe statistical differences in the skin deformation between compliant pairs before they are perceptually discriminable. For example, at a depth of 1 mm and velocity of 1.75 mm/s, the eccentricity cue is distinct for all four compliant pairs at 0.6 s, even though only the 45/10 kPa pair is perceptually discriminable, Fig. 2.3C. Second, we observe the force cue is distinct only for the less compliant 184/121 kPa pair, Fig. 2.3D, whereas the perceptual predictiveness of the contact area cue is mixed, Fig. 2.3E. Indeed, with this approach we observe differences in skin deformation at early time durations, before they are perceptually discriminable. However, several issues arise in using this approach to tie the skin deformation cues with the perceptual outcomes. In particular, it cannot differentiate if perceptual differences are informed by the skin cues at that given observation's time point or accumulated over multiple prior time points. If only individual time points are evaluated, then no time history information is included, yet Fig. 2.2 indicates that time duration and velocity impact perception. For this reason, we sought a second approach to evaluate how the cues evolve over time, in line with prior works [55]–[57].

Approach 2: change rate of skin deformation over the time course of the indentation

In a second approach to comparing the skin deformation cues and perceptual judgments, we evaluated change rates in the cues, per indentation, over the time course of the indentation. In this way, the single estimate produced per indentation is made, and then compared with that of the other stimulus of the pair.

An example application of this procedure is given in Fig. 2.4. Fig. 2.4A-B describes forming a singular estimate of the magnitude for a first stimulus, then an estimate of a second stimulus, so to difference those estimates to generate a single discriminability estimate, Fig. 2.4C. In particular, the change rates of contact area for 45 and 10 kPa stimuli at 1.75 mm/s velocity are calculated as 48 mm^2/s and 67 mm^2/s, Fig. 2.4A. Over the series of change rates representing the entire time course of an indentation, the middle value in the sequence is selected. The median value was used, rather than the mean, to better represent the central tendency over the indentation and be robust to outliers given the distribution of our datasets. Next, in Fig. 2.4B, these median change rates at the 1.75 mm/s velocity, and at all velocities, are plotted. Building up further, Fig. 2.4C shows the contact area rate difference from Fig. 2.4B for this 45/10 kPa compliant pair, and all compliant pairs across all velocities. The results in Fig. 2.4C indicate that the contact area rate difference decreases as velocity increases, especially for the 45/10 kPa compliant pair. Also, the order of the stimulus pairs in Fig. 2.4C, with 45/10 kPa first, then 35/5 and 184/121 kPa, and 75/45 kPa follows discrimination results in Fig. 2.2. In effort to statistically correlate the skin deformation cues with the perceptual judgments, we performed a regression analysis. A subset of the perceptual results for two indentation velocities are plotted in Fig. 2.4D, with contact area rate differences in Fig. 2.4E. Then regression is performed between these two variables, Fig. 2.4F-G. The results indicate that the contact area cue well correlates with perceptual discrimination across the compliant pairs and indentation velocities, with R^2 values greater than 0.7. Correlations for cues of contact area, as well as curvature, force and eccentricity, are summarized in Fig. 2.4H. Interestingly, the curvature cue exhibits high correlation with the perceptual results for the more compliant pairs (33/5 and 45/10 kPa). In contrast, the force cue exhibits high correlation for the less compliant pairs (184/121 and 75/45 kPa), while the eccentricity cue is well correlated at the extremes of the compliant pairs away from the stiffness of the skin (184/121 and 33/5 kPa pairs). The rate difference data that underlies these cues can be found in Appendix, Fig. A3. Indeed, it indicates that the difference in the curvature change rates decreases with velocity only for the more complaint pairs (33/5 and 45/10 kPa); the difference in force rates decreases for the less compliant pairs (184/121 and 75/45 kPa); and decreases for eccentricity for all except the 45/10 kPa pair.

Moreover, as associated with the results in Fig. 2.4H, we conducted a one-way ANOVA to evaluate the dependency of overall rate difference in skin deformation cues on discrimination performance per compliance pair, across all velocities. The results indicate that perceptual discrimination is significantly associated with differences for contact area for all compliant pairs ($F_{1,175}$ = 19.6, p < 0.05 for 184/121 kPa pair, $F_{1,175}$ = 22.1, p < 0.01

for 75/45 kPa pair, $F_{1,174} = 88.8$, $p < 0.001$ for 45/10 kPa pair, $F_{1,174} = 27.2$, $p < 0.01$ for 33/5 kPa pair), whereas curvature is correlated with discrimination only for 45/10 kPa ($F_{1,174} = 30.1$, $p < 0.001$) and 33/5 kPa ($F_{1,174} = 16.3$, $p < 0.05$) pairs, compared to the force cue, which is only significant for the less compliant pairs ($F_{1,175} = 25.8$, $p < 0.01$ for 184/121 kPa pair, $F_{1,175} = 26.3$, $p < 0.01$ for 75/45 kPa pair), and the eccentricity cue has an impact on perception for 184/121 kPa ($F_{1,175} = 49.0$, $p < 0.001$), 75/45 kPa ($F_{1,175}= 31.2$, $p < 0.001$), and 33/5 kPa ($F_{1,174} = 20.9$, $p < 0.05$) compliant pairs.

In summary, correlations between skin surface deformation and perceptual judgements are observed across the stimulus compliance and indentation velocity. However, the highest correlations are observed between rate differences in contact area, which are consistent across all compliances and velocities. Moreover, curvature exhibits high correlation for the more compliant stimuli, force for the less compliant stimuli and eccentricity for the most and least compliant stimulus pairs. The utility of the force cues with less compliant stimuli, in particular, align with prior psychophysical studies which have utilized for stiffer stimuli [11], [31], [37], [58], [59]. The eccentricity cue, which describes the contact shape, has been found to be correlated with percept of friction [60]. The work herein supplements such with results with more information on the utilization of cues for predicting perception regarding factors of stimulus compliance, indentation velocity and depth.

Dependency between skin deformations cues

As indicated in Fig. 2.4H, the perceptual results may be associated with more than a single cue, e.g., for the less compliant 184/121 kPa pair, where both contact area and force are strong predictors. Therefore, we evaluated the degree of independence between the cues in statistical correlations conducted across stimulus compliance, indentation velocity and depth, using Pearson correlation. Of all the cues in Fig. 2.5, only one, penetration depth, relatively highly correlates with other cues, in particular curvature ($r = 0.70$, $p < 0.001$) and contact area ($r = 0.62$, $p < 0.001$), in agreement with prior works [11]. The low degree of correlation between the other cues implies that the cues are not statistical dependent, indicating together with Fig. 2.4 that we indeed may utilize more than just one skin deformation cue to form perceptual judgements.

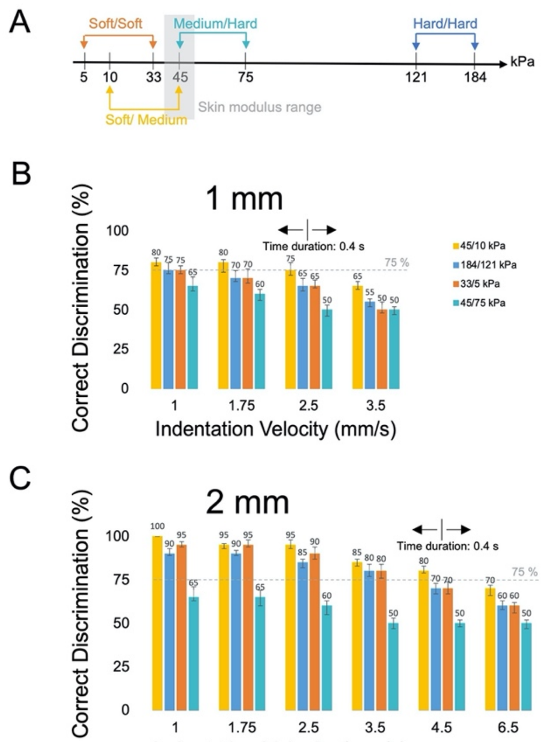

Figure 2.2. Psychophysical evaluation of compliant pairs across indentation depths and velocities. In panel **(A)**, four compliant pairs were selected to be more compliant than that of the skin (33/5 kPa), less compliant than skin (184/121 kPa) and overlapping (75/45 and 45/10 kPa). Skin stiffness is about 42 – 54 kPa. **(B)** Pairwise perceptual evaluation of stimuli indented sequentially into the passive index finger pad to 1 mm depth at four indentation velocities, resulting in time durations of 1, 0.56, 0.4, 0.3 s. **(C)** Stimulus indentation to 2 mm depth at six indentation velocities, resulting in time durations of 2, 1.14, 0.8, 0.56, 0.4, 0.3 s. The findings indicate that the compliant pairs are not discriminable before a time duration of 0.4 s. Beyond that time point, pairs delivered at higher velocities are more difficult to discriminate. The 45/10 kPa pair is the most discriminable and the 75/45 kPa pair is not discriminable above a level 75% for any indentation velocity.

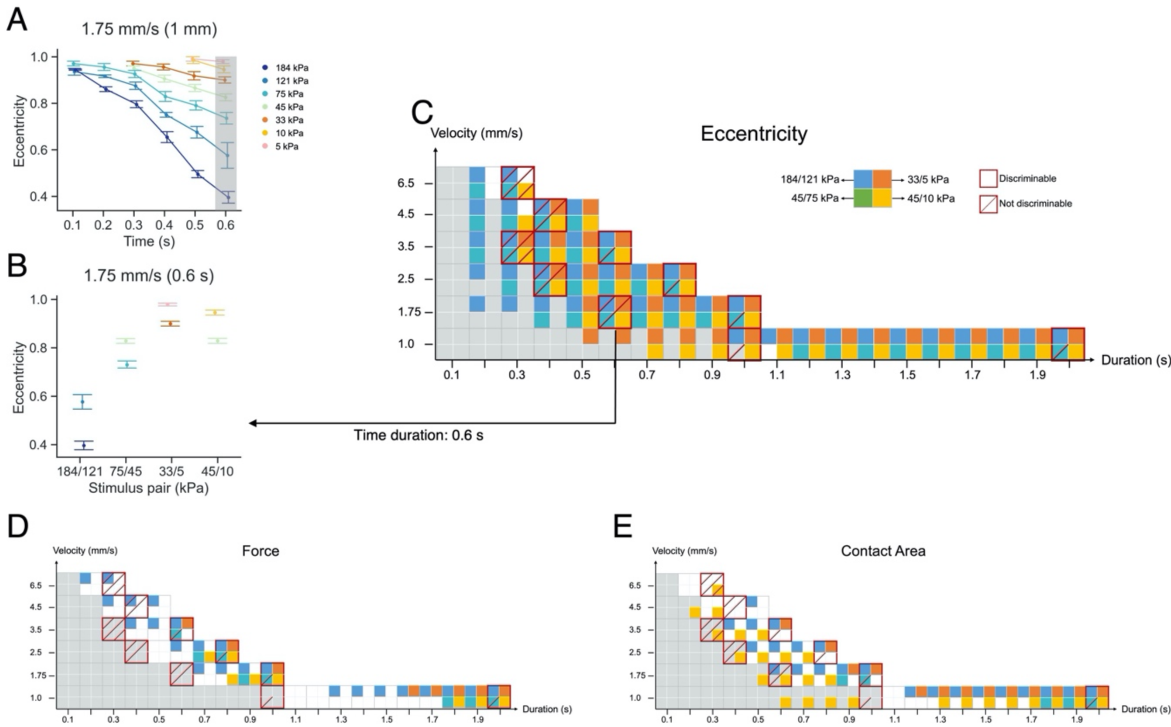

Figure 2.3. Using Approach 1 to compare skin deformation cues calculated at discrete time points with the perceptual results, across the compliant pairs, indentation velocities and displacements. As a unit, panels **(A-C)** describe the approach 1 process for the eccentricity cue. **(A)** Observations for eccentricity over the time course of indentation for the seven stimulus compliances at a velocity of 1.75 mm/s and displacement of 1 mm. **(B)** The four compliant pairs at 0.6 s from panel (A). **(C)** An evaluation of statistical significance for these four compliant pairs, where each block represents an evaluation of a compliant pair, and the use of colored block, as opposed to the gray or white framework, indicates statistical significance. Blocks in the framework with a grey background represent a stimulus displacement of 1 mm and a white background 2 mm. Moreover, blocks outlined in red indicate compliant pairs where psychophysical experiments were conducted, with open blocks being perceptually discriminable above 75% and a crossed-out blocks represent a lack of discriminability at that level. These data come from Fig. 2. For the eccentricity cue, the blocks in **(C)** indicate that all four compliant pairs are statistically different, yet only the 45/10 kPa pair is perceptually discriminable. Panel **(D)** shows the results for force cue which is more distinct for the less compliant pairs, and **(E)** shows the results for contact area cue which indicates mixed results. In summary, Approach 1 does not lead to clear connections between any of the cues and the perceptual outcomes.

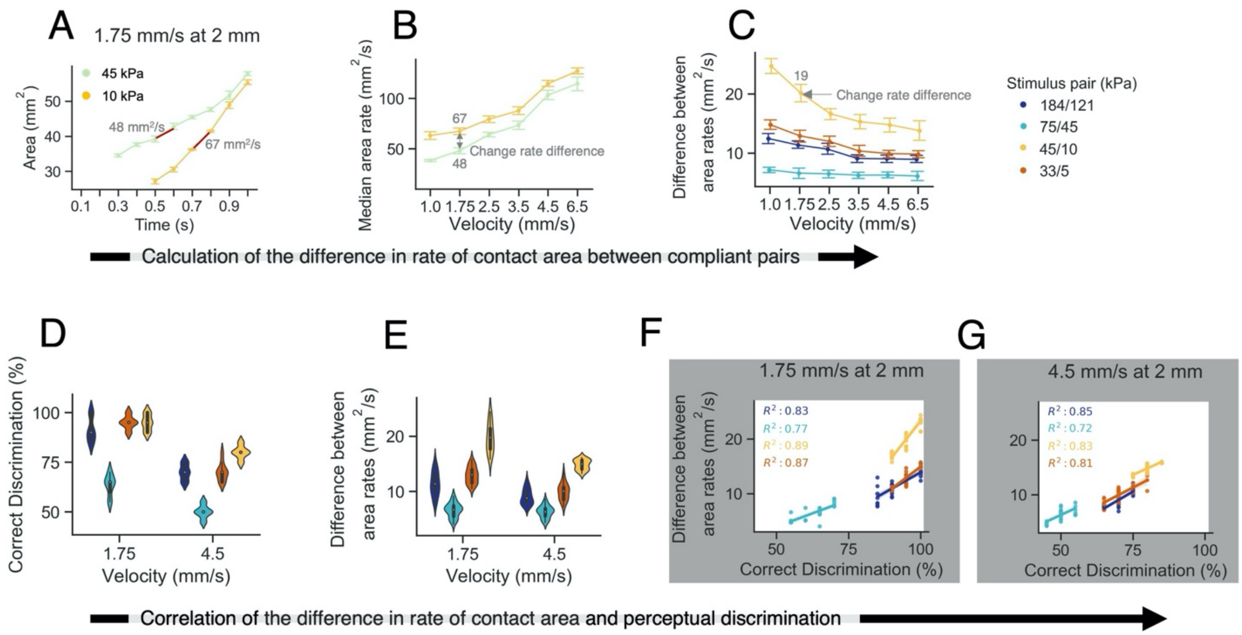

H

Pairs (kPa) \ Cues (R^2)	Area	Curvature	Force	Eccentricity	
184/121	0.83	0.32	0.91	0.75	— 1.75 mm/s at 2 mm
	0.85	0.42	0.82	0.70	— 4.5 mm/s at 2 mm
75/45	0.77	0.46	0.75	0.66	
	0.72	0.53	0.71	0.59	
45/10	0.89	0.76	0.37	0.52	
	0.83	0.72	0.50	0.58	
33/5	0.87	0.89	0.22	0.74	
	0.81	0.88	0.43	0.71	

Figure 2.4. Using Approach 2 to compare the difference in rate of change in contact area between compliant pairs with discrimination performance. (**A-B**) An example of the steps in calculating the rate differences in contact area, from discrete time points to change rate across six velocities. Change rates of contact area for 45 and 10 kPa stimuli at 1.75 mm/s velocity are calculated, with median values of 48 mm^2/s and 67 mm^2/s. Change rates at all velocities are plotted. **(C)** The contact area rate difference for the 45/10 kPa compliant pair, as well as all compliant pairs across all velocities, showing a decrease with increased indentation velocity. The error bar is computed using bootstrapping, showing estimates of the true mean and 95% confidence. **(D)** Psychophysical discrimination results from Fig. 2 for the four compliant pairs at 1.75 and 4.5 mm/s velocities, and **(E)** corresponding differences in contact area rate differences from (C). **(F-G)** Regression associates contact area rate difference with discrimination per compliance pair, with correlations listed. **(H)** Summary of the correlations of all skin deformation cues, with those higher than 0.7 are highlighted in gray. In summary, high correlations between rate differences in contact area are observed across all compliances and velocities, while curvature exhibits high correlation for the more compliant stimuli, force for the less compliant stimuli, and eccentricity for the most and least compliant stimulus pairs.

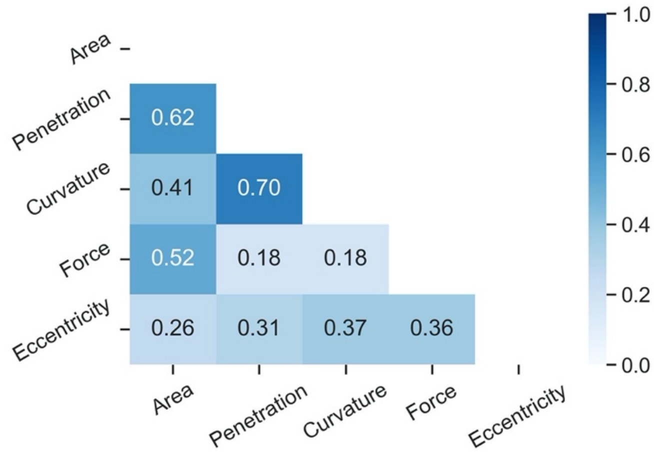

Figure 2.5. Evaluating the degree of independence between the skin deformation cues (change rates from Approach 2). Only the penetration depth cue exhibits a relatively high correlation with curvature ($r = 0.70$, $p < 0.001$) and contact area ($r = 0.62$, $p < 0.001$). The low degree of correlation between the rest of cues implies statistical independence.

Discussion

As we go about daily interactions with soft and compliant objects, the neural afferents innervating our skin signal patterns in its surface deformation. Such patterns are shaped by the compliance of a contacting object relative to the skin's stiffness, as well as its indentation velocity, depth, and duration. This work sought to better understand both how compliant stimuli are encoded in patterns of deformation at the skin's surface and how such patterns may be correlated with evoked percepts. These are fundamental topics in somatosensory perception and prerequisites in designing haptic actuators and rendering algorithms.

Herein, we conducted human-subjects experiments with a custom-built 3-D stereo imaging system to observe the skin through transparent, compliant stimuli. The results show that a minimum contact duration of at least 0.4 s is required for perceptual discriminability. Beyond that point, compliant pairs delivered at higher velocities are increasingly difficult to discriminate, in agreement with smaller changes in skin deformation. In a detailed quantification of the skin's surface deformation, we find that several, independent cues aid in the discrimination of compliant pairs. In particular, we find that temporal changes in the gross contact area well correlate with discriminability, regardless of stimulus compliance and indentation velocity. However, other independent cues tied to surface curvature, eccentricity, and bulk force are likely complementary in informing perceptual judgements, in certain situations, e.g., bulk force when a contacting object is less compliant than the skin itself.

Indentation duration and velocity shape discrimination

We find that a contact duration of 0.4 s is required for perceptual discriminability. This observation is robust across combinations of indentation depths and velocities, which vary the stimulus duration between 0.3 – 2.0 s, Fig. 2.1B-C. In particular, the 45/10 kPa pair is discriminable in two cases where time duration is 0.4 s, both a velocity of 2.5 mm/s and indentation depth of 1 mm, and at 4.5 mm/s and 2 mm, indicating that the duration of the indentation is impactful beyond its velocity alone. At constant depths of indentation, slower velocity results in longer duration contact, which has been shown to facilitate a greater accumulation of information [56], [57]. With a shorter duration of contact, the relatively weaker contribution of the first stimulus makes it more difficult to discriminate from the second stimulus. Interestingly, in terms of observations of skin deformation, in particular contact area, we begin to observe pairwise differences between the 45/10 kPa stimulus pair slightly earlier, at 0.3 s.

The study's experimental paradigm also varied the velocity of the indentation ramp from 1 – 6.5 mm/s to evaluate its effects on skin deformation and perception. We observe a greater degree of perceptual discriminability between compliant pairs at the slower velocities, Fig. 2.2B-C. Discriminability was reliable across three compliant pairs at 1 mm/s for the 1 mm depth and 3.5 mm/s for the 2 mm depth. Likewise, we observed greater differences in the skin's deformation between compliant pairs at slower velocities, in particular, for the contact area rate cue, Fig. 2.4C, but also for the curvature, eccentricity and force rate cues (Appendix, Fig. A2). Moreover, at velocities of 1.75 mm/s and 4.5 mm/s, the skin deformation cues, in particular the change rate of contact area between compliant pairs are well correlated with rates of perceptual discrimination, Fig. 2.4H. Indeed, prior studies have indicated that indentation velocity can influence neural firing and our perception of compliance [47]–[49]. For instance, LaMotte and Srinivasan found the discharge rate of neural afferents increases monotonically with velocity. As denoted by our findings herein, we extend these efforts by defining the contributions of those skin deformation cues that are most robust at reliably encoding object compliances across a range of indentation velocities.

The utility of distinct skin deformation cues

In a detailed quantification of the skin's surface deformation, we find that several cues independently aid in the discrimination of compliant pairs. Among the five skin deformation cues, the change rate of contact area over the indentation is most highly correlated with perceptual judgments. In particular, large differences in this cue between compliant pairs were observed across the full range of object compliances, which well correlate with rates of perceptual discrimination (R^2 values of 0.72 to 0.89), Fig. 2.4H. That said, other cues related to skin surface curvature and bulk force were correlated with perceptual judgments, for stimuli more and less compliant relative to the skin, respectively, Fig. 2.4H. In this way, the findings indicate that the change rate of contact area is a very useful all-around cue, though not per se at static or terminal snapshots in time. Compared to prior work which has pointed to the utility of contact area cues [5], [4], [6], [41], we distinguish its rate of change. Encoding via a rate of change metric also appears to be important in accounting for individual differences in skin properties [4], [39], [41], and in active touch, where volitional movements are made to optimize force rate while minimizing object deformation [11], [37].

The magnitudes of contact area measured in this study align closely with prior efforts using both rigid [12], [61], [62] and elastic [5], [11], [50], [52] stimuli in passive touch. In particular, using an ink-based technique, Hauser and Gerling measured the contact area as about 80 and 65 mm^2 when the finger pad was indented by 120 and 22 kPa stimuli at a 2 mm depth, respectively. Similarly, the measurements in this study range from 78 mm^2 for 121 kPa and 54 mm^2 for 10 kPa stimuli. Similarly, Dzidek et al. estimated contact areas of about 90 and 100 mm^2 at forces of 1 and 1.5 N, when the finger was indented by a rigid plate at a 30-degree angle, which is close to our measurements of 83, 89 mm^2 for the 184 kPa stimulus that has a lower modulus than a rigid plate [12]. That stated, one should note that magnitudes of contact area measured in the literature can vary significantly to the differences in experimental setup, such as finger contact angle and stimulus geometry.

In addition to contact area, other skin deformation cues appear to be fruitful dependent on object compliance relative to the skin. Herein we evaluated the discriminability of four compliant pairs (184/121, 33/5, 45/10, and 45/75 kPa), whereby the 184/121 kPa pair was less compliant than skin, and 33/5 kPa was more compliant than skin, and the remaining pairs spanned the skin's modulus in either direction. The results indicate unique patterns in skin deformation. For example, in Fig. 2.4, with the highly compliant 45/10 kPa pair, we observed the best correlation with perceptual judgments for contact area and curvature, whereas for the less compliant 184/121 kPa pair, contact area and force produce the highest correlation. These findings also hold when the cues are evaluated at discrete time points using Approach 1, Fig. 2.3. In comparison with prior literature, our measurement of force is about 0.75 N at 1 mm/s velocity for a soft stimulus (45 kPa), similar with 0.7 N at 0.5 mm/s for compliant stimuli [10], [59], and our results also align with the perceptual utility of the force cue for less compliant stimuli [11], [31], [37], [58], [59]. Indeed, most prior studies use stiff stimuli, relative to skin [53], and for this reason may be distorting our understanding of a broader range of compliant interactions. Furthermore, we note that the compliant pairs at equal 30 kPa intervals, i.e., 33/5 and 75/45 kPa, exhibit different rates of discriminability and preferred skin deformation cues. This distinction indicates a sensitivity to objects more compliant than the skin that is perhaps ecologically driven. Although further work is necessary to fully define the non-linearities in touch relative to stimulus modulus, such perceptual tuning aligns with psychophysical findings in audition.

Discrimination strategies for rate-based encoding

Two approaches were developed to compare skin deformation cues and perceptual judgments. In particular, with our imaging setup, we evaluated skin deformation cues at discrete observation time points (Approach 1) as well as by their change rates over the indentation (Approach 2). We found that cues associated with the latter approach better correlated with discriminability. Over the series of change rates representing the entire time course of an indentation, our approach used the middle value in the sequence. This was done, rather than using the mean, to represent the central tendency of the data over the indentation and to be robust to outliers. Other approaches could have averaged or summed the data or accumulated change rates in a temporally weighted manner.

Others have employed somewhat similar approaches. For example, Xu et.al (2020) evaluated the dissimilarity between force rates based on the discrete time differences in discriminating between naturalistic objects, and found a correlation with perceptual performance [55]. Indeed, memory representations in discriminating compliance are affected by exploration length and temporal delay in which haptic information is gathered and integrated in a continuous manner [56], [57]. Further efforts, likewise, have shown that temporal-based cues such as accumulative discrete-time difference and average change rate difference, are largely correlated with perceptual discrimination [11], [36], [39], [41], [51], as opposed to cues defined at terminal indentation [4]–[6]. Additional efforts will be required to refine the nature of how information is accumulated over time in order to arrive at judgments.

Aim 2: Evaluate the impact of individuals' skin properties on their tactile discriminability

Introduction

Tactile acuity varies among individuals and declines over one's lifespan, as influenced by fingertip size, skin stiffness, age, gender, and cognitive factors. Declines related to aging intertwine several causes [63]–[66]. In contrast, in younger age cohorts, finger size alone has been correlated with acuity [17], [18], [67], [68]. The current working hypothesis is that the density of neural afferents determines perceptual acuity. Given that individuals generally have the same number of afferents, smaller fingers lead to higher afferent density and superior ability [18]. Therefore, women, due to smaller fingers on average, tend to demonstrate higher tactile acuity than men. However, as has been noted in Peters, et al. (2009), observed inter-individual variance in tactile acuity remains yet unexplained even upon accounting for finger size.

In addition to his or her finger size, an individual's skin mechanics may influence tactile acuity. For instance, in cases of age-related degradation, decreased tactile sensitivity has been observed with changes in skin mechanics, apart from changes in cognitive functioning [19], [69], [70]. Indeed, such reductions in tactile acuity may result from a loss of elastin fibers and increased wrinkling of the skin [71]. Moreover, aging women tend to experience decreased skin thickness, which also reduces tactile acuity, and in a much more dramatic way than for aging men [71], who start with larger and thicker finger pads, due in part a thicker stratum corneum [18]. Furthermore, and most evident when isolated in younger people in their 20s and 30s, increased skin conformance (a measure of how much the skin invades the gaps in grating stimuli) is associated with lower tactile detection thresholds [20], [21], [72]. Some have suggested that increased skin conformance may increase neural firing rates of afferents responding to edge stimuli (13), though the results yet remain inconclusive [74]. How such changes in the skin's mechanics influence perceptual discrimination remains unanswered. In addition to skin stiffness, fingerprint ridge breadth may play a role. In particular, the dense papillary ridges of the skin are filled with sweat ducts and sites of afferent innervation [71], [75]–[77] while underlying and opposing intermediate ridges are sites where changes in the stiffness of skin layers may amplify the response sensitivity of originating afferents, especially slowly adapting type I fibers [78], [79].

Herein, we decouple the impact of three skin properties, including fingertip size, skin stiffness, and fingerprint ridge breadth, on individual differences in perceptual acuity in younger participants. In analyzing these factors, 3-D stereo imaging is used to capture the deformation of the skin surface over the time course of stimulus indentation, perceptual discrimination is evaluated across a robust and naturalistic range of object compliances, and hyaluronic acid is used to soften the skin to directly modulate its stiffness for perceptual evaluation.

Material and Methods

Participants

A total of 40 young participants were recruited (mean = 28, range = 21 – 32, 19 males and 21 females). None had prior experiences with discrimination tasks nor reported a history of finger injury. Their fingers were free of calluses and scars. A written, informed consent was obtained from each participant before conducting the experiments which were approved by the local institutional review board. After used by a participant, all devices and surfaces were sanitized.

Stimulus fabrication

As a reference, the average compliance of human fingers is about 42 kPa [80], [81]. Seven elastic stimuli were fabricated with compliance ranging from 5 to 184 kPa, in which one stimulus (45 kPa) was close to human finger compliance, with three stimuli were softer (5, 10, 33 kPa) and three harder (75, 121, 184 kPa). Each silicone-elastomer was poured into an aluminum collar (5.4 cm outer radius by 1.6 cm depth) fitted and sealed with a clean, dry glass disc (5.1 cm radius by 0.3 cm depth) using a syringe tip filled with 0% diluted Solaris, heated at 100 Celsius until fully sealed. To formulate the more compliant stimuli (5,10,33 kPa), a two-component silicone rubber (Solaris, Smooth-on Inc., Macungie, PA, USA) was mixed at ratio of 1:1, diluted by silicone oil (ALPA-OIL-50, Silicone oil V50, Modulor, Berlin, Germany) with ratios of 200 wt.% for 33 kPa, 300 wt.% for 10 kPa and 400 wt.% for 5 kPa. Each mixture was placed in a vacuum chamber under 29 mmHg for 5 minuets then rested in room temperature until all bubbles were released. Next the transparent mixture was cured in an oven at 100 Celsius for 25 minuets to fully solidify before returning to room temperature. To eliminate surface stickiness caused by high dilution ratio, a thin layer of 100% diluted Solaris silicone rubber was applied on the stimulus’s surface, then cured at 100 Celsius for 15 minuets. For the rest of stimuli (45, 75, 121, 184 kPa), a different two-component silicone rubber (Sylgard 184, Dow Corning, Midland, MI, USA) was used and diluted by silicone oil with ratios of 200 wt.%, 100 wt.%, 50 wt.% and 0 wt.%, respectively.

Measurements of finger skin properties

Finger size. The length and width of distal phalanx of the index finger were used to estimate participants' finger size. The length is measured as the distance between fingertip edge and DIP joint, and the width is the distance from left to right edge of the finger, where they intersect the center of finger pad. Then finger size is estimated as the area of an ellipse which is formed by the length as its major axis and width as the minor axis.

Finger stiffness. The finger stiffness is typically measured by a rigid body compression test [82]. A glass plate (5.4 cm radius by 0.3 cm depth) is indented in the index finger at a rate of 1 mm/s, while simultaneously measuring force. The stiffness is approximated as the slope of linear regression of the force-displacement curve at 2 mm displacement. Since contact area, determined by finger size, modulates compressive force measured by the load cell and in turn potentially influences the measurements of finger stiffness, we investigated the statistical correlation between finger stiffness and the contact area at 0.3 seconds which is within the linear region of force curve, shown in Appendix 1(c). The results indicate that contact area does not have significant effect ($R = 0.27$, $p < 0.001$) on the measurement of finger stiffness.

Finger ridge breadth. During the indentation by a glass plate, the image of finger was captured by the camera and the contact surface between skin and glass plate was extract, shown in Fig. 3.2(f). To obtain a clear representation of fingerprint lines, we applied a localized thresholding filter (OpenCV, Python 2.8) with adjusted contrast and brightness in the grayscale image, shown in Fig. 3.1(b). Then we applied the same approach used in [83] ,where the ridge breadth is measured as the length of a line that across ten parallel ridges with no minutiae causing a break in the perpendicular line, indicating by the red dash line. Furthermore, we converted the units from pixels to millimeters, illustrated in Appendix A1 (a)-(b).

Psychophysical experiments

A series of discrimination tasks were designed and conducted to evaluate the participants' discrimination ability in compliance. Four pairs of stimulus comparison were prepared: 45/10, 184/121, 33/5 and 75/45 kPa, where 184/121 kPa pair is less compliant than the skin, and 33/5 kPa pair is more compliant than the skin, and the remaining pairs span the skin's modulus in either direction. During the experiment, the participant was seated in an adjustable chair and the finger was placed directly under the substrate. A blindfolder was provided to eliminate any visual cue throughout the experiments. For each pair, each stimulus was sequentially delivered to the participant's index finger in randomized order for a total of 20 trails. We also delivered the same stimulus twice to the finger to test the individual biases. After indented by two sequential stimuli, the participant was asked to report which of the two stimuli was more compliant, either the first or second. The switching time between two stimuli was about 2 s. In total, there were 4,000 indentations, consisting of 2 stimuli within a pair, 4 comparison pairs, 20 trails, and 25 participants. The average duration of this experiment per participant was about 80 minuets including breaks. We conducted the psychophysical experiments before biomechanical experiments for two reasons: one is to maintain a consistent time interval between two stimuli, as in biomechanical experiments the stimulus surface needs to be cleaned after each indentation (3-5 s); and the other reason is to ensure a greater cognitive attention from the participants.

Biomechanical experiments

During the experiment, seven compliant stimuli were delivered to the finger individually at a rate of 1.75 mm/s at 2 mm displacement, repeated 3 times for each stimulus. A thin layer of ink was applied on the finger using a paint brush with its bristles normal to the skin surface. Before indentation, each stimulus was brought into the finger with a light contact force (< 0.1 N) then slowly retracted to 0 N to ensure a consistency in initial contact states between trails. The ink residuals were removed after each indentation to attain the highest quality of imaging data. In total, there were 525 indentations, consisting of 7 compliant stimuli, 3 repetitions and 25 participants. The average time to complete this experiment was about 70 minuets including breaks.

Skin stiffness modulation

A new group of 15 participants were recruited in this experiment, and their skin properties information is not included in the previous analysis. To modulate the skin stiffness, a few drops of hyaluronic acid serum (Cosmedic skincare Inc. Rocklin, CA), an agent that helps relax and hydrate the skin, was applied on the fingertip skin and waited to dry at room temperature. We measured the participants' skin stiffness and evaluated their perceptual performance before and after the treatment the same way as described above.

Statistical analysis

To divide the participants into subgroups based on their finger size, stiffness and ridge breadth, we used k-means clustering method (n = 25). Clusters of two appeared to be optimal using the elbow method in which the sum of squared distance between each point and the centroid in a cluster was plotted with number of clusters, shown in Appendix A2. Principal component analysis (PCA) was used to assess the differences in use of deformation cues between two groups. The total explained variances from the first and second principal components for each cue were summed and compared for each group, shown in Fig 3.5(c).

Next, we employed multivariant regression model for each group to predict the discrimination performance across participants based on their finger properties. The data was split into a training set (75%) and a test set (25%). The independent variables were the change rate of five skin deformation cues and the dependent variable was the correct discrimination from the psychophysical experiments. To validate the use of regression models, we checked that the independent variables were not statistically dependent, and the residuals were randomly distributed, in Appendix A3. We used 10-fold cross validation to build subgroup models (n = 1050 in Group 1 model, n = 945 in Group 2 model), and values of R^2 and RMSE were used as evaluation parameters for the model performance.

Results

Through a series of biomechanical, psychophysical, and statistical modeling experiments, this work shows that an individual's skin stiffness alone well predicts their ability to perceptually discriminate compliant objects, by evoking more prominent distinctions in their skin surface deformation at the point of contact. First, relationships are evaluated between measurements of fingertip size, skin stiffness, and fingerprint ridge breadth, and each in turn with perceptual discrimination. Second, imaging is used to characterize patterns, or cues, in the deformation of the skin's surface, using a 3-D stereo technique. Third, measurements of skin deformation indicate how the finger properties (stiffness, size, and ridge breath) modulate levels of discrimination, respectively. Then, statistical models are used to decouple fingertip size and stiffness and characterize the performance of two distinct subgroups of participants, which do not divide entirely upon gender lines, but are driven more so by an individual's skin stiffness. Finally, hyaluronic acid is applied to soften the skin stiffness of a new cohort of participants with pre- and post-test of perceptual performance.

The results show that finger size and stiffness are positively correlated, and those who have smaller and softer fingers achieve higher perceptual performance. Biomechanical cues in the deformation of the skin surface are highly correlated with perception, in particular the rate of change in contact area, and we observe that softer fingers generate larger differences in contact area between pairs of stimuli, leading to better discriminative performance. Consequently, finger stiffness is more correlated with such skin cues than is finger size, indicating that stiffness is more effective in modulating local skin deformation. Moreover, by changing an individual's skin stiffness directly, while finger size remains constant, the discriminative ability of each participant is shown to improve, especially those beginning with the stiffest skin.

Experiment 1: Relationships between finger properties and perceptual discrimination

Perceptual discrimination of material compliance is evaluated in passive touch via pairwise comparison. Four compliance pairs are used, 45/10, 184/121, 33/5 and 75/45 kPa, Fig 3.1(a). The 45/10 kPa pair is readily discriminable by all participants, while the 75/45 kPa pair is not discriminable at a threshold of 75% correct. Between these extremes, both the 33/5 and 184/121 kPa stimulus pairs are discriminable. Note that the compliance values of these two pairs were selected as they more certainly lie to either side of the skin's stiffness, observed to be approximately 42 - 54 kPa [53], [80]. Moreover, we were aware that participants might experience learning phenomenon as they were getting more familiar with the tasks which could improve their discrimination correct rate. We compared the psychophysical performance across five trails for a male and a female participant, shown in Appendix 4 (a)-(b). We found that there was no noticeable difference in discriminability between trails, indicating that the learning phenomenon does not have significant on the participant's perceptual judgement.

The finger properties of each participant, including fingertip size, skin stiffness and fingerprint ridge breadth, were measured, as detailed in Methods, with variance observed across the cohort. As indicated in Fig 3.1(b), the male participants of this study spanned a range of finger widths of two standard deviations (mean = 18 mm) as compared with the literature [84], while that for female participants lied closer to the average value (mean = 15 mm) within one standard deviation. A high correlation was observed between fingertip size and skin stiffness (R^2 = 0.9, p-value < 0.001, SE = 2.96 x 10^{-4}), with less significant correlation between either of these metrics and fingerprint ridge breath, Fig 3.1(c). Fingerprint ridge breadth is correlated with finger size (R^2 = 0.76, p-value < 0.001, SE = 9 x 10^{-4}), as noted similarly in prior works [75], [76], and was positively correlated with stiffness (R^2 = 0.7, p < 0.001, SE = 4.4 x 10^{-3}).

When the three finger properties are each correlated with perceptual performance in the compliance discrimination task, skin stiffness exhibits the highest correlation across stimulus pairs (R^2 = -0.95, -0.93 and -0.77 for 184/121, 33/5 and 75/45 kPa pairs), followed by finger size (R^2 = -0.91, -0.82 and -0.65) and ridge breadth (R^2 = -0.81, -0.70 and -0.43), respectively, Fig 3.1(d)- (f).

Experiment 2: Characterization of skin surface deformation

Local patterns in the deformation of the skin surface constitute the major factor driving our percept of compliance [1], [85]. To evaluate if certain cues in the skin's deformation align with both correct discrimination and one or multiple finger properties, we image 3-D high-resolution profiles of the skin's surface using techniques described previously [39], [51], [86], Fig 3.2. Basically, images taken by the two cameras through transparent, compliant substrates are used to construct a 3-D point cloud which represents the geometry of finger pad at the contact surface. This is done for the seven stimuli ranging from 5 to 184 kPa. From the point cloud data, we evaluate five derived biomechanical cues to characterize the surface's deformation over time, which include contact area, curvature, penetration depth, eccentricity and force [51].

From representative point cloud data in Fig. 3.3, one can observe that the skin deforms differently with respect to stimulus compliance as well as finger stiffness. Indented by a less compliant stimulus (184 kPa, row 3 in Fig. 3.3(a)), the finger pad's surface flattens against the substrate, which generates higher contact area and force with a more circular contact shape. In contrast, with a more compliant stimulus (45 kPa, row 1 in Fig. 3.3(a)), the finger pad's surface relatively retains its shape and penetrates into the substrate, which produces higher curvature and penetration depth with a more elliptical contact shape. Moreover, an individual's skin stiffness affects the way the skin surface deforms. For instance, when the more compliant stimulus (45 kPa) is indented into softer skin (0.097 N/mm), we observe greater contact area as opposed to stiffer skin (0.152 N/mm), Fig. 3.3(a) rows 1 and 2, and Fig. 3.3(b), green lines. In comparison, for the less compliant stimulus (184 kPa), finger stiffness appears to have less impact on contact area, Fig. 3.3(b), blue lines. However, such trends in contact area do not follow with cues such as penetration depth, or for force with the more compliant 45 kPa stimulus.

Experiment 3: Individual differences in finger properties modulate skin deformation and perceptual discrimination

Though skin stiffness is highly correlated with perception, are the distinctions in the skin deformation cues, and perceptual discriminability of compliant pairs, sensitive to the changes in finger stiffness? To address this question, we first compared the change rates in the skin deformation cues between stimulus pairs with their corresponding rates of correct discrimination as our perception is more tied with the rate-based cues rather than the change itself, Fig 3.4(a)- (b). The change rate is defined as the median value from a sequence of change rate calculated at a 0.1 s time interval, indicated as a red line segment in Fig 3.4(a) for 184 and 121 kPa stimuli with median change rates of 34 mm^2/s and 41 mm^2/s in contact area, respectively. Agreed with prior work which has shown that the change rate of contact area is highly tied to perceptual discrimination of compliance [4]–[6], the results show that two of the cues, i.e., change rates of contact area and eccentricity, are highly correlated with the perceptual discrimination across the cohort of

25 participants in distinguishing between 33/5 and 184/121 kPa stimulus pairs. Whereas the change rates of force and curvature are correlated with perception for the less compliant pairs (184/121 and 75/45 kPa) and more compliant pair (33/5 kPa), respectively.

Then we evaluated how finger stiffness, size and ridge breadth influence the change rate of contact area and force, represented in Fig 3.4(c)- (d). Across either cue of contact area or force, skin stiffness is the most highly correlated of the finger properties, in agreement with Experiment 1, Fig. 3.1(c). Indeed, softer skin generates larger distinctions in skin deformation, in particular in its contact area change rate (r^2 > 0.9 for 45/10, 33/5 and 184/121 kPa pairs), which are correlated with higher rates of perceptual discrimination, regardless of fingertip size. On the other hand, stiffer fingers generate higher force rate compared to soft fingers, but the difference in force rates becomes smaller as the skin stiffness increases, as shown in Fig 3.4(d).

Experiment 4: Decoupling the impact of fingertip size and skin stiffness on perceptual discrimination in subgroups of participants

Fingertip size and skin stiffness have been found to be highly correlated and both contribute to perception acuity by tuning skin deformation at the point of contact surface. Meanwhile, two groups are observed differing in their skin properties. Thus, we developed statistical models to decouple the effect of fingertip size and skin stiffness on perceptual acuity and evaluate the performance of subgroups. Two distinct groups are identified based on three skin properties (size, stiffness and ridge breadth) using K-means method, in Fig 3.5(a). Even though the groups seem to be mostly separated by genders, those males who have small or soft fingers are categorized as in Group 1 which contains the females who in general have smaller and softer fingers. The performance evaluated from the psychophysical tasks is compared and found to be significantly different between these two subgroups, even for 75/45 kPa stimulus pair which is not discriminable, in Fig 3.5(b). Moreover, we observe that the skin deforms differently for each group using principal component analysis (PCA), indicating Group 1 which contains small and soft fingers favors skin cues such as contact area, penetration depth and curvature, whereas Group 2 which contains large and stiff fingers rely more on the force and eccentricity cues, shown in Fig 3.5(c). Additionally, the discriminability seems to be affected by skin properties within subgroups. Six participants are selected from the groups, indicated by the numbers in Fig 3.5(a), and their performance is individually compared. As expected, participant 1 who has the smallest and softest finger, has the highest correct discrimination, in Fig 3.5(d). When the fingertip size is similar but skin stiffness varies (participant 3,4 from Group 1), lower skin stiffness leads to a higher discriminative performance. In contrast, when the skin stiffness is similar but fingertip size varies (participant 2,3 from Group 1 and participant 5,6 from Group 2), a large increase in size does not necessarily result in a higher performance. This observation is aligned with Experiment 3 suggesting skin stiffness affects perceptual discrimination more than fingertip size does. Indeed, by using multivariant regression modeling that used to predict the discriminative performance from skin properties, the results indicate that an individual's perceptual abilities can be readily predicted based on their skin stiffness alone, shown in Fig 3.5(e).

Experiment 5: Decreasing skin stiffness improves one's perceptual discrimination

Another way to decouple fingertip size and skin stiffness is to change one's skin properties. It is unlikely to change someone's finger size, however, the skin stiffness can be modulated. Thus, to further investigate if skin stiffness plays a more dominate role than fingertip size on tactile acuity, we directly soften the skin stiffness by applying hyaluronic acid for a new cohort of participants (n=15). Two distinct groups are separated by the skin stiffness and their psychophysical performance is evaluated before and after modulating the skin surface. The results show that the participants' skin stiffness can be largely reduced by applying hyaluronic acid on the skin surface, in Fig 3.6(a). And their discrimination performance is observed to be significantly improved after reducing skin stiffness, especially for those with stiffer fingers (participant 9-15), Fig 3.6(b). Furthermore, the overall performance across participants for each group is also statistically improved for 75/45 kPa pair in Group 1 and for all three pairs in Group 2, as shown in Fig 3.6(c). The results speculate that at both individual and aggregated level, reducing skin stiffness results in a higher perceptual performance. In sum, this experiment has shown that skin stiffness can be modulated, and by changing one's skin stiffness directly, while fingertip size remains constant, the discriminative performance is shown to be markedly improved which reinforces the finding that skin stiffness is more influential than fingertip size in affecting perceptual acuity.

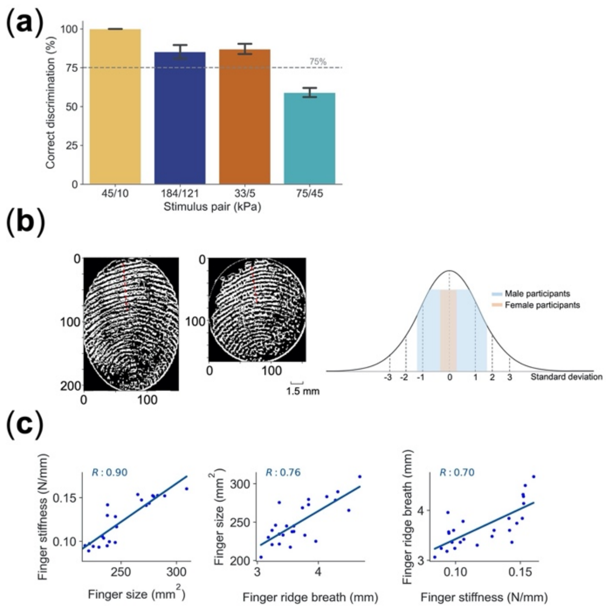

Figure 3.1. Relationships between fingertip skin properties and perceptual discrimination. (a) Psychophysical performance in pairwise discrimination of compliant stimuli indicates that the 45/10 kPa pair is discriminable always, the 184/128 and 33/5 kPa pairs are each discriminable above a 75% correct threshold, and the 75/45 kPa pair is not discriminable at this threshold. (b) Left: Fingertip contact with a glass plate for two example participants from which ridge breath measurements were derived. Right: Overlay of the finger width of this study's male and female participants on a large-sampled dataset of 4000 people (25). (c) Relationships for each participant between their finger size, stiffness, and ridge breath, indicating the highest correlation between finger stiffness and size. (d) – (f) Relationships between the participants' perceptual discrimination performance and skin properties. The highest correlation is observed for finger stiffness, then finger size, and ridge breath.

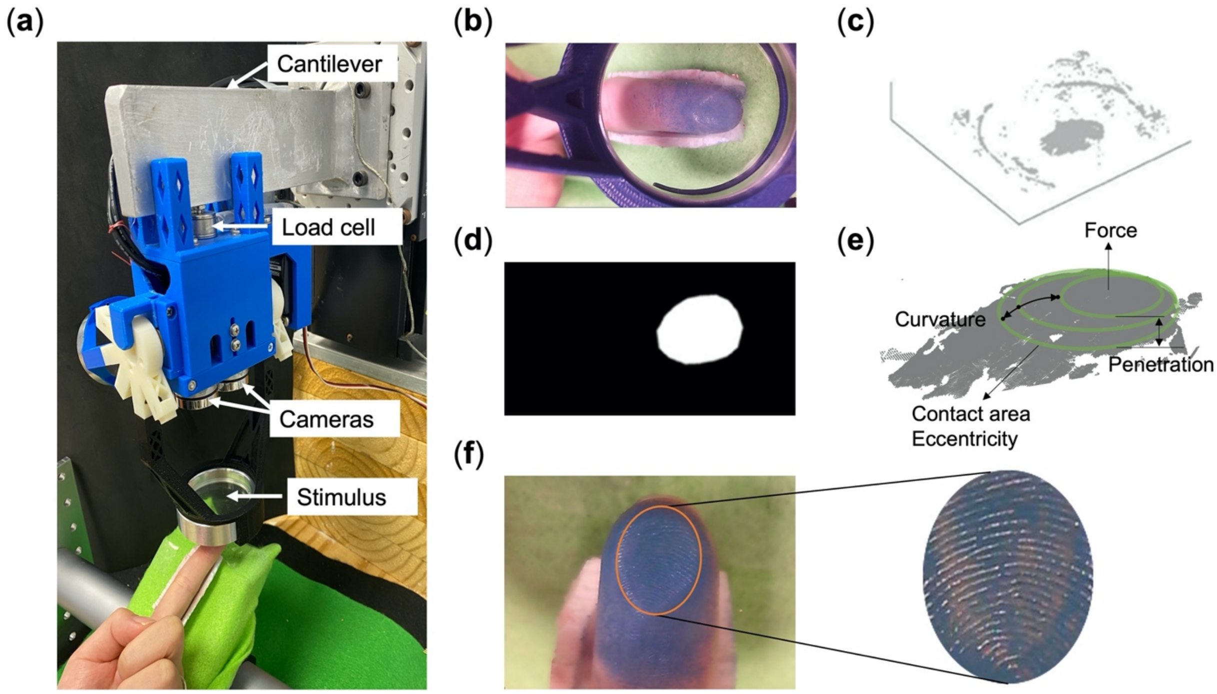

Figure 3.2. Experimental setup to generate 3-D point clouds for evaluating finger skin properties and deformation. (a) A mechanical-electrical indenter delivers elastic, compliant substrates to the fingertip. (b) The left image of fingertip indented by a 45 kPa substrate at 2 mm displacement. (c) A 3-D point cloud is constructed from left and right images of the finger using a disparity-mapping algorithm. (d) The region of contact between the skin and substrate is manually selected by masking. (e) A clean point cloud that represents the skin surface is generated, ellipses are fitted to reduce its dimensionality, and five skin cues quantify patterns of deformation. (f) A glass plate is used to measure each participant's fingertip stiffness and ridge breath.

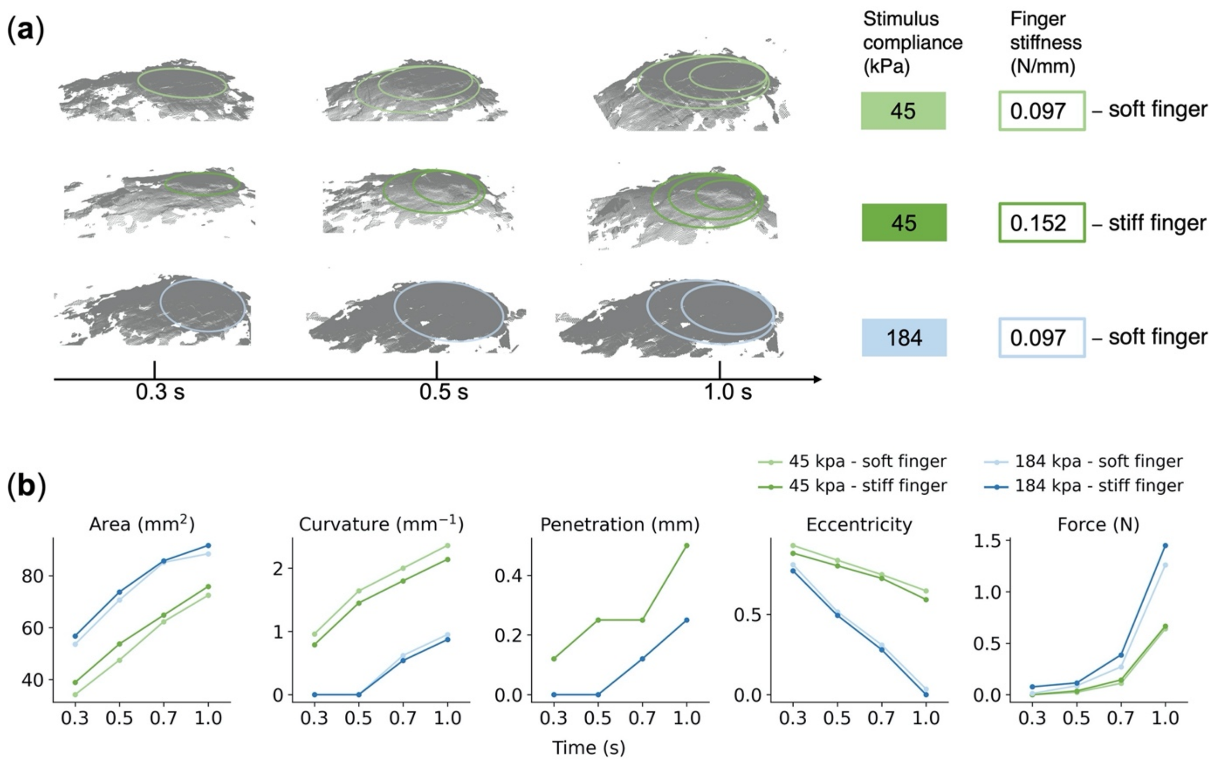

Figure 3.3. Time-evolution of skin surface deformation for two exemplar stiff and soft fingertips indented by 45 and 184 kPa compliant stimuli at a rate of 1.75 mm/s to 2 mm displacement. (a) Changes over 0.3, 0.5, and 1 seconds of the 3-D point cloud that represents the skin surface, when stiff and soft fingertips make contact with more (45 kPa) and less (184 kPa) compliant stimuli. (b) Comparisons of five skin deformation cues between these two participants and two stimulus compliances. Contact area as well as the other cues differ between stimulus compliance. In terms of participant finger stiffness, when a more compliant stimulus (45 kPa) is indented into the skin of each participant, we see the curves differ for contact area, curvature, and eccentricity, though not penetration or force. In contrast, for those three metrics, finger stiffness has less impact on skin deformation when indented by less compliant stimuli (184 kPa), although the force cue becomes differentiable. These example cases are subsequently quantified and statistically evaluated across a population of participants.

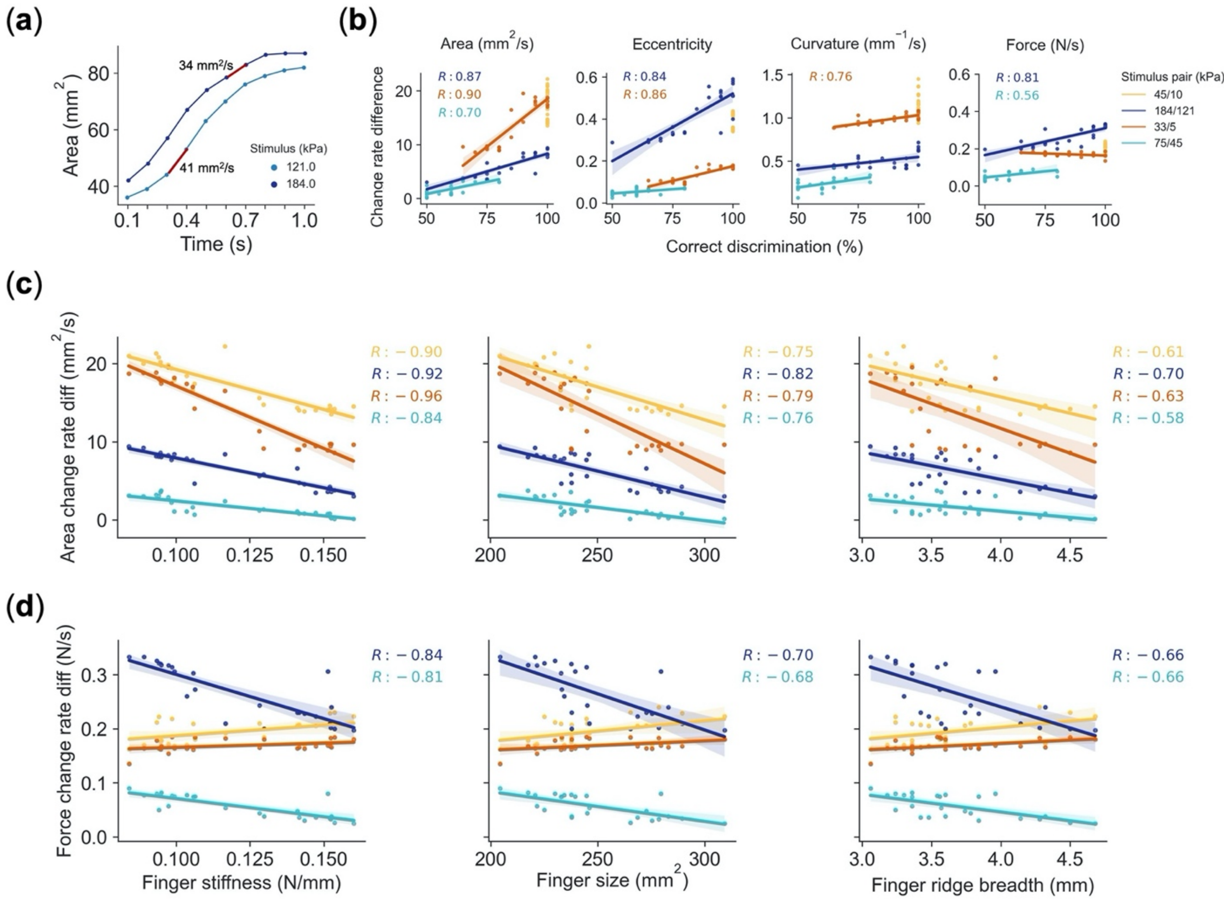

Figure 3.4. Relationships between the skin deformation cues (change rate differences) for stimulus pairs and correct perceptual discrimination as well as the fingertip property of stiffness, size and ridge breadth. Four colored lines represent the stimulus pairs. (a) An example of the steps in calculating the change rate in contact area from discrete time points. Change rate of contact area for 184 and 121 kPa stimuli are calculated, with median values of 34 mm^2/s and 41 mm^2/s, respectively. The rate difference of 7 mm^2/s is then plotted as a data point in (b). (b) Contact area and eccentricity change rate shows high correlations with discrimination in differentiating between 184/121, 33/5, and 75/45 kPa stimulus pairs, in contrast to the other three cues. (c) Finger properties are negatively correlated with contact area change rate, in particular, finger stiffness shows the highest correlation, followed by size and ridge breadth. (c) Finger stiffness is also highly correlated with force change rate for 184/121 kPa stimulus pair, indicating a dominate role in modulating local skin deformation that drives discrimination perception.

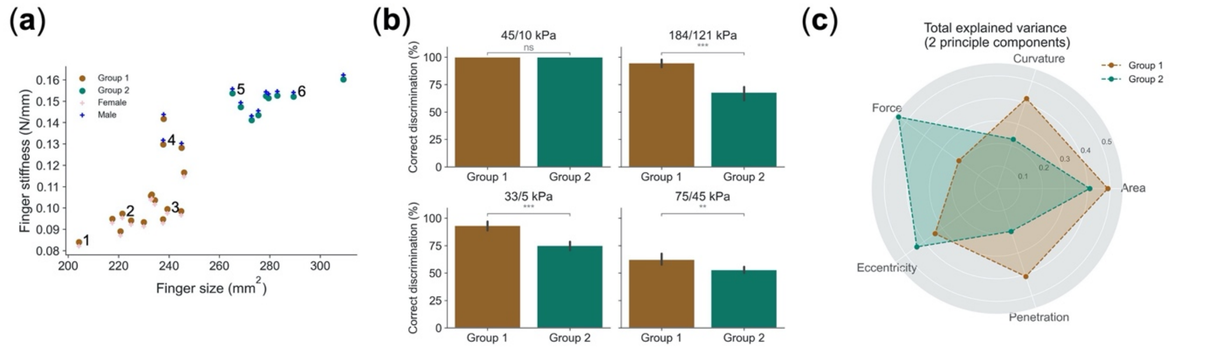

(d)

	Correct discrimination (%)			
Participants	45/10	184/121	33/5	45/75
1	100	100	100	80
2	100	100	100	75
3	100	100	95	65
4	100	85	85	50
5	100	70	80	50
6	100	65	75	60

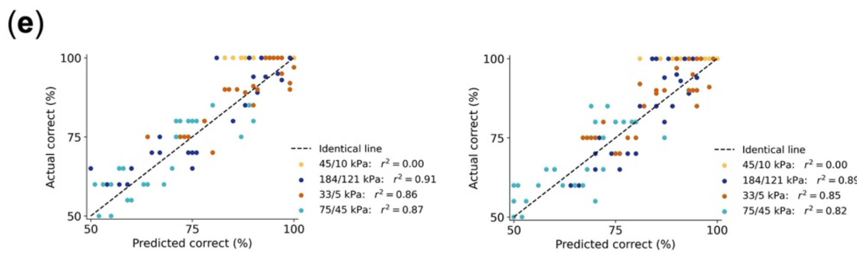

Figure 3.5. Multivariant regression models show that the participants can be separated into two distinct groups and that discrimination performance can be well predicted from one's finger stiffness alone. (a) Using a K-means approach, the cohort of participants is clustered into two groups based on their finger size, stiffness, and ridge breath. This clustering reveals that for the most part, though not entirely, these are groups of male and female participants. (b) Statistical comparisons in perceptual discrimination between these two groups ($p < 0.05$), showing these two groups performed significantly different in the discrimination tasks. (c) Differences in skin deformation cues between two groups using PCA analysis, indicating that those in Group 2 (stiffer finger skin) rely more on force cues. (d) Six participants from the groups (4 participants from Group 1 and 2 participants from Group 2) are selected and their discrimination performance are compared, showing the performance is affected by finger properties within the clusters. (e) Evaluation of model performance when the discrimination is predicted by the three factors of finger size, stiffness, and ridge breath versus predicted by finger stiffness alone. Small improvements in prediction are achieved by adding the other two factors.

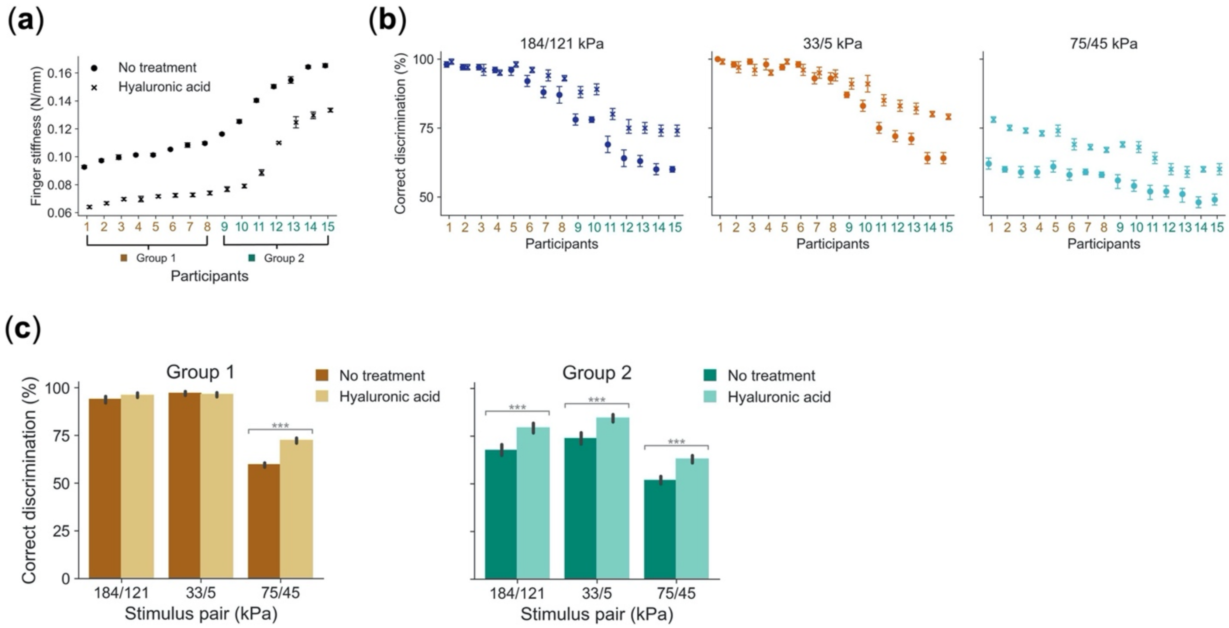

Figure 3.6. The finger stiffness of 15 new participants is modulated by applying hyaluronic acid on the skin surface and the discrimination performance is significantly improved by decreasing the finger stiffness. Two distinct groups are separated based on their finger stiffness before the treatment using K-means algorithm. (a) compares the finger stiffness before and after applying hyaluronic acid, per participant. (b) shows the discrimination performance of three stimulus pairs before and after applying hyaluronic acid, per participant. Participants are arranged with increasing finger stiffness where participant 1 has the softest finger and participant 15 has the stiffest finger. (c) shows that the overall performance between treatments is compared statistically for three stimulus pairs, indicating that the performance is largely improved by decreasing the finger stiffness.

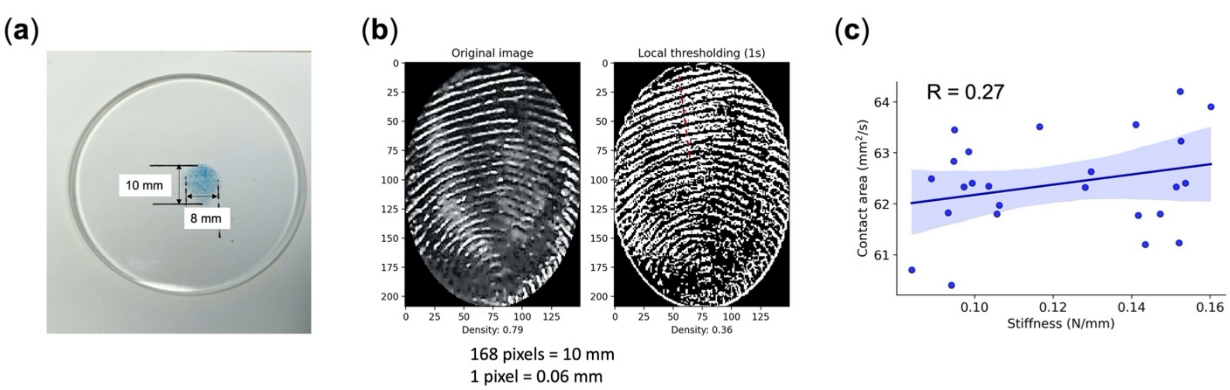

Appendix 1. Steps of measuring finger pad ridge breadth. (a) contact region between the skin and a glass plate from the compression test, the length and width are measured by a digital caliper. (b) Correlate the physical measurements with digital images. (c) Validation of the effect of contact area on the measurements of finger stiffness.

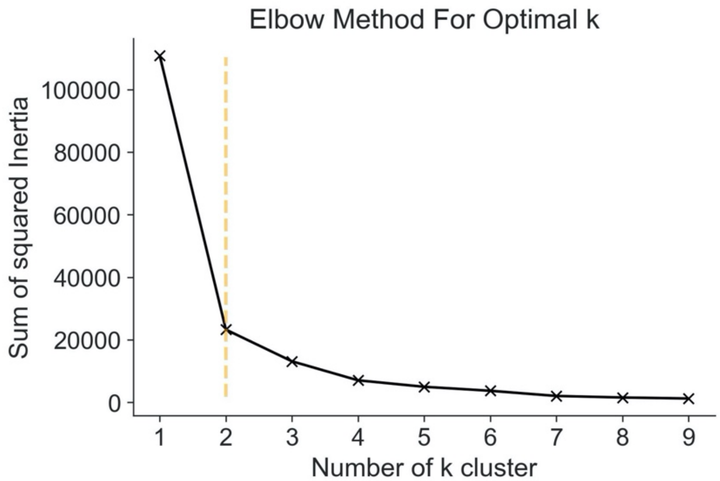

Appendix 2. Choice of the number of clusters in K-means algorithm. The elbow effect occurs at k = 2.

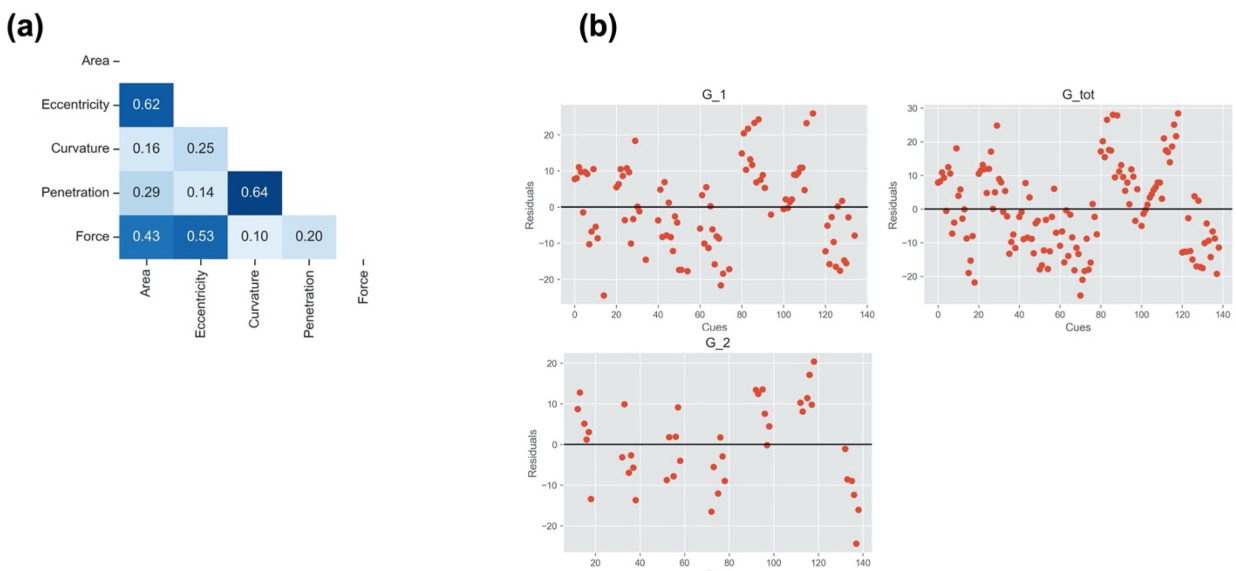

Appendix 3. Assumption check for the linear regression model. (a) statistical dependency between the independent variables which are the change rate of contact area, eccentricity, curvature, penetration depth and force. (b) the residuals from the linear model are randomly distributed which validate the use of such model.

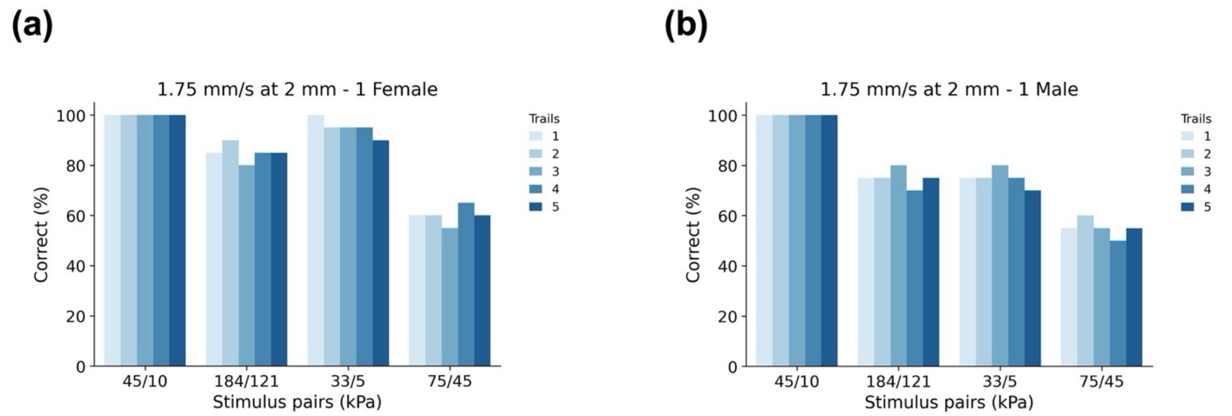

Appendix 4. Evaluation of psychophysical bias caused by learning phenomenon. The discrimination performance is compared across five trails for (a) a female and for (b) a male participant, at 1.75 mm/s indentation velocity. The results indicate that there are no significant perceptual biases in the psychophysical experiment.

Discussion

This work is one of the few studies that access individual differences in compliance discrimination by investigating the finger properties and skin deformation. Usually, finger size is found to be associated with tactile perception, however, we observed that finger stiffness is at least as influential as finger size in discriminating compliance by modulating local skin deformation. We also found certain skin cues are more effective than others in capturing skin deformation as well as relating to perception, such as contact area. Moreover, we found that one's perceptual discrimination can be well predicted by finger stiffness alone.

Importance of finger stiffness in predicting individual discrimination performance

Tactile acuity is known to be declined with increasing finger size as larger fingers tend to have a lower density of mechanoreceptors given there is no significant difference in total number of afferents across males and females [18], [67], [75]. The impact of gender on acuity can be explained by the physical differences between the fingers of males and females, that is women who on average have smaller fingers have higher receptor densities, which result in a better perception [18], [20], [68], [71]. In this study, we found that those who have small fingers also tend to have soft fingers, and they outperform those have big and stiff fingers in the discrimination tasks. Finger stiffness is found to significantly influence local skin deformation and perceptual responses. Thus, addition to finger size which contributes to innervation density, finger stiffness can also affect tactile perception by modulating skin deformation which in turn varying the firing rate and population of afferents, and moreover it shows a stronger statistical correlation in predicting perception than finger size does. To hypothesize that a superior tactile perception comes from a lower finger stiffness not smaller size, we compared the perceptual performance between two participants who shared similar finger size but different stiffness (participant #3,4), also between two participants who shared similar finger stiffness but different size (participant #2,3) in Fig 3.5(a). The results show that the performance is significantly lower with higher finger stiffness, but smaller finger does not largely improve the performance when finger stiffness is about the same. Indeed, in the literature there are studies investigating the relationship between skin modulus and perceptual acuity. Hamasaki et.al developed a finite element model for human finger that contains the simulation of stratum corneum, a tissue determines skin stiffness. The results indicate that changing skin stiffness would influence tactile perception by affecting the stress distribution around Merkel Cells [22]. Woodward (1993) found no significant correlation between skin compliance and perceptual acuity, however, Gibson and Craig (2006) argued that such insignificance might have resulted, given the force-controlled paradigm used, from an insensitivity to forces greater than 50 g whereas tactile sensitivity is largely affected between 0 and 25 g. Moreover, attempts have been made to directly change skin stiffness by applying venous occlusion to the finger pulp [74], which significantly influences the firing activities of rapidly adapting mechanoreceptors. Similarly, researchers have observed that by hydrating the fingertip skin, contact area can be largely increased [87] which aligns well with our findings that softer fingers afford a higher degree of skin deformation which allows more information collected at the local contact.

Two distinct participant groups (can be used to approximate) that predict discrimination performance

Individual differences in touch behavior have been often neglected by research [88], nonetheless, some studies observed that people exhibit different preference based on their motivation and ability to use haptic information, evaluated by the Need for Touch scale (NFT) [89]. For example, people with high NFT tend to feel more confident in exploring objects when haptic information is available; women shows a higher need for tactile input than men in making product evaluations [90]; for those who are motivated to touch, a communication that incorporates sensory feedback leads to increased affective response and persuasion [91]. Those examples show that individual differences are observed in touch behaviors across a population, but also can be classified based on their need of haptic information.

In this work, we observed individual differences in tactile perception and two groups of participants were found in distinction of finger properties and discriminability, in which their discrimination performance can be predicted by the finger stiffness. Yet, how exact to draw the line in assessing individual differences still needs further investigation, in other words, at what level we should care about individual differences. For example, we might observe more than two distinct groups if more participants were recruited and vice versa. Moreover, as this work is only focused on the perception in compliance, we do not know how meaningful perceptual differences will be presented in other attributes and tasks.

Skin deformation cues useful as a surrogate for neural population response

Our sense of perception is provoked by the activities of afferents embedded under our skin, transmitting local skin deformation into sensory signals for perception. The current technique is limited to record single unit afferent response, and by now, it is nearly impossible to get afferents population responses due to the technical and ethical issues even though some efforts have been done to access afferents population activities using Calcium imaging for mice, but not for humans [92]. Therefore, skin cues are developed and found to be associated with afferents responses that drive our perceptual responses, such as contact area [4], [5], penetration depth [6], [93] and contact force [7], [8]. In this work we observed certain cues are more effective than the others in capturing skin deformation but also in predicting perceptual discrimination, shown in Fig 4. Additionally, we found that people with different finger properties utilize different skin cues which has not been reported in the literature. For example, those who have stiffer fingers tend to use force cue whereas those with softer fingers prefer curvature and penetration depth cue.

Changing skin mechanics state influences perception

Studies have shown that changing skin mechanics may have impact on tactile perception. Hudson (2015) inspects the responses of cutaneous mechanoreceptors before and after using venous occlusion to change the finger stiffness. The results show that increasing stiffness of the skin affects the firing rate of SA II type afferents, however, weather such effects can alter perceptual discriminability still remains unanswered [74]. Moreover, even if the change in skin mechanics affects perception, does it adjust our behavior and decisions as well? Indeed, in active touch where the force and displacement are not constrained, people are observed to choose different strategies to achieve optimal discrimination. In particular, for those who have stiffer fingers, they tend to apply higher force and larger displacement when differentiating compliant objects [1]. From this insight, our future work leads to investigate the changes in participants' discrimination behaviors mechanics in an active touch paradigm when the skin mechanics is altered. Specifically, we can compare the force, displacement and reaction time utilized by the participants before and after the skin modulation.

Aim 3: Design soft haptic actuators to visualize the finger pad surface at distinct percepts of compliance

Introduction

Our perception of compliance, or softness, plays an essential role in object manipulation and social interaction. Yet how compliance is encoded at the cutaneous skin surface remains ambiguous. In general, our somatosensory system relies on a variety of mechanosensitive afferents that are activated by patterns of deformation, which is quantified in terms of skin surface cues such as contact area [4]–[6]. Such cues can predict perceptual performance [39], [93], [94]. However, in order to fully understand the utility of particular skin cues on the perception of compliance, efforts are needed to directly control the skin surface while simultaneously monitoring it.

Several prior efforts have developed reconfigurable haptic displays to simulate compliant interactions. One class of devices optimizes the movement of rigid surfaces [95]–[98]. Another uses elastomers and other soft materials that conform to the shape of the finger and change its geometry [99]–[101]. For instance, hydraulic and pneumatic mechanisms can inflate and displace an membrane's surface, and in turn deform the skin's surface [23], [24], [26], [102]–[104]. Properly configured, these actuators can generate vertical displacements of 3 mm and forces of 1 N [23]. Dielectric elastomers have also been adopted to induce tactile patterns, but the range of protrusion is relatively limited due to high voltages [32], [105]. Also, external stimulus-responsive actuators can modulate their stiffness via particle jamming [106], [107] and have used smart materials such as magnetorheological particles and hydrogels [29], [108], [109].

Yet in few of these compliant, conformable, and reconfigurable actuators can one directly assess the resultant deformation of the skin surface. Indeed, evaluation of their performance is limited to perceptual judgments. To directly observe the skin during actuation, transparent soft actuators have been built, but with limited mechanical actuation force, e.g., 0.25 to 300 mN, and surface displacement of less than 1 mm [24], [110]–[112]. Moreover, few of devices have sought to mimic skin cues, such as change in contact area, which is correlated with perceptual discriminability [6], [39]. Conversely, other devices can regulate contact area and indentation depth [23], [103], [113], [114] but are unable to directly assess the actual deformation of the skin surface.

In contrast, this work describes the design and evaluation of a transparent, reconfigurable, multi-channel hydraulic actuator. The transparency of this actuator enables the observation of skin deformation profiles concurrently during actuation. These profiles are used in the evaluation of the actuator in addition to perceptual judgments. Overall, by directly observing the skin surface through the actuated channels, the intent is to introduce a testbed capability, as opposed to a consumer device, to decipher cutaneous cues that drive perception, by precisely controlling and replaying them.

Material and Methods

Fabricated of transparent elastomer, the actuator contains a pattern of discrete concentric ring channels pressurized by fluids of similar refractive index. Profiles of the contacting skin surface can be directly visualized through actuated channels to match observations with solid substrates. First, the actuator is fabricated by selecting its mechanical structure, material, and channel filler. Then, its mechanical performance is evaluated at different actuation states in terms of channel displacements and contact forces. Next, we perform 3-D imaging through the actuator to reconstruct skin surface geometry and deformation. Finally, biomechanical experiments compare patterns of skin deformation obtained between the actuator and solid elastic substrates. Perceptual discriminability across configured levels of stimulated moduli is evaluated and compared to levels deemed discriminable with standard solid elastic stimuli.

Fabrication of transparent, multi-channel actuator

Three primary factors were considered in selecting the actuator material: elasticity, transparency and de-moldability. Solaris silicone rubber was chosen to construct the actuator, due to its low viscosity, optical clarity and high elongation at break (290%). To further increase its compliance, we diluted the elastomer with silicone oil at a 100% ratio. Demolding the actuator was a significant challenge due to the complex milli-fluidic structures and small distance between channels. After iterating on various mold materials and geometries, we created a custom machined aluminum mold that employs optimized minimum channel dimensions (1.25 mm width, 1.5 mm height, 1.5 mm wall thickness), Fig. 4.1A-left. The actuator is comprised of two bonded elastomer layers with the actuation control ports in the bottom layer (Fig. 4.1A-right). The four actuator channels are dual-ended and arranged in an elliptical shape mimicking the finger pad. Each channel can be actuated independently for localized control and minimized crosstalk. A cross-section through the actuator midline in Fig. 4.1B reveals the channel geometry and 0.5 mm thick actuator surfaces.

The detailed fabrication steps are as follows: First, the silicone-elastomer solution is prepared by mixing silicone rubber (Solaris, Smooth-on Inc., Macungie, PA, USA) with the curing agent at a ratio of 10:1, and then diluted with silicone oil (ALPA-OIL-50, Silicone oil V50, Modulor, Berlin, Germany) at a ratio of 100% (1:1 ratios of silicone rubber to oil). Second, a thin layer of mold release agent (Mann Release Technologies, Inc., Macungie, PA, USA) is sprayed upon the aluminum plate and dried at room temperature. Then, the diluted PDMS solution is slowly poured into the mold, avoiding trapping extra air during the process. The mold is transferred to a vacuum chamber for 3 min at 25 inHg until the air bubbles release and is then cured at 70 C for 20 min. Once the bottom and top layers are solidified, they are carefully demolded from the aluminum plate using a micro spatula. Undiluted Solaris is then used as an adhesive agent for connecting the layers, tubes, and glass substrate.

Once constructed, the final step was to select a filler fluid for the channels. When filled with air, the channel edges appear visible, causing light glare and introducing imaging noise. Ideally silicone oil would be used, however it can degrade the silicone-elastomer. Propylene Glycol (PG) was found to be an appropriate filler fluid having a similar density (1.04 g/cc) and refractive index (1.43) with the actuator elastomer (density = 0.99 g/cc, refractive index = 1.41) without damaging the silicone-elastomer. After filling the channels, their edges are much less visible, Fig. 4.1C-D.

Validation of actuator mechanics and transparency

<u>*Evaluation of channel displacements and forces.*</u> The vertical displacements of individual channels were measured by an electric caliper (FunOwlet Tech. Co., Shenzhen, China), while the inside pressure level was monitored simultaneously with a digital pressure gauge (Tekcoplus Ltd, Kowloon, Hong Kong, China). The force-displacement characteristics of the actuator at different pressurization states were compared with solid substrates of known modulus. For this, an electro-mechanical motion controller and load sled with two stereo cameras was used for delivering the actuator to an individual's index finger pad at a rate of 1.75 mm/s and indentation depth of 2 mm [51], [115], [116]. During indentation, contact force was measured by the load cell at 150 Hz with a resolution of ±0.05 N (LCFD-5, Omegadyne, Sunbury, OH, USA).

<u>*Evaluation of actuator transparency*</u>. First, a rigid cylinder's surface (radius 10.7 mm) was imaged through both the actuator and a transparent, solid stimulus to calculate the spatial variation from the ideal. After either was indented into the object, a disparity-mapping

algorithm was used to construct a 3-D point cloud representing the object's surface geometry [115]. The point cloud was generated by co-locating ink points applied on the object's surface (and later the finger pad) from the images captured by the left and right cameras (Papalook PA150, Shenzhen Aoni Electronic Industry Co., Guangdong, China), at 30 frames per second, with a maximum resolution of 1280 by 720 pixels. The dimensionality of the point clouds was reduced by fitting the scatter points into vertically stacked ellipses [51].

Validation of actuator with human-subjects

Participants. A total of five participants (mean age = 28, 3 males and 2 females) were recruited. The experiments were approved by the local Institutional Review Board, and informed consent was obtained from all participants. During the psychophysical experiments, participants were blindfolded to eliminate visual cues.

Biomechanical experiments. The ability to image through the actuator was evaluated by indenting the index finger to 2 mm with channels filled by air or PG fluid, then using the disparity-mapping method to generate a point cloud data for comparison. Then, we reconfigured the actuator to three states at which the force-displacement characteristics are equivalent with solid substrates of 33, 45, and 75 kPa compliances. As well, we imaged through the transparent, solid substrates. Furthermore, we extracted four previously defined cues (contact area, curvature, eccentricity, and force) that describe the skin deformation profile at each actuation state, for comparison with the solid substrates [39], [51].

Psychophysical experiments. We evaluated the discriminability of pairwise configurations of the actuator, at simulated compliances of 33, 45 and 75 kPa. A configured actuator was indented to the participant's index finger at a rate of 1.75 mm/s and depth of 2 mm, with a 2 sec interval between the pair. Each pairwise comparison was delivered five times, and the order of the pairs was randomized. Participants reported which of the pair was more compliant, first or second. In total, there were 150 indentations, consisting of the 2 in a pair, 3 comparison pairs, 5 repetitions and 5 participants. The average time per participant to complete the experiment was 30 min, with a 10 min break.

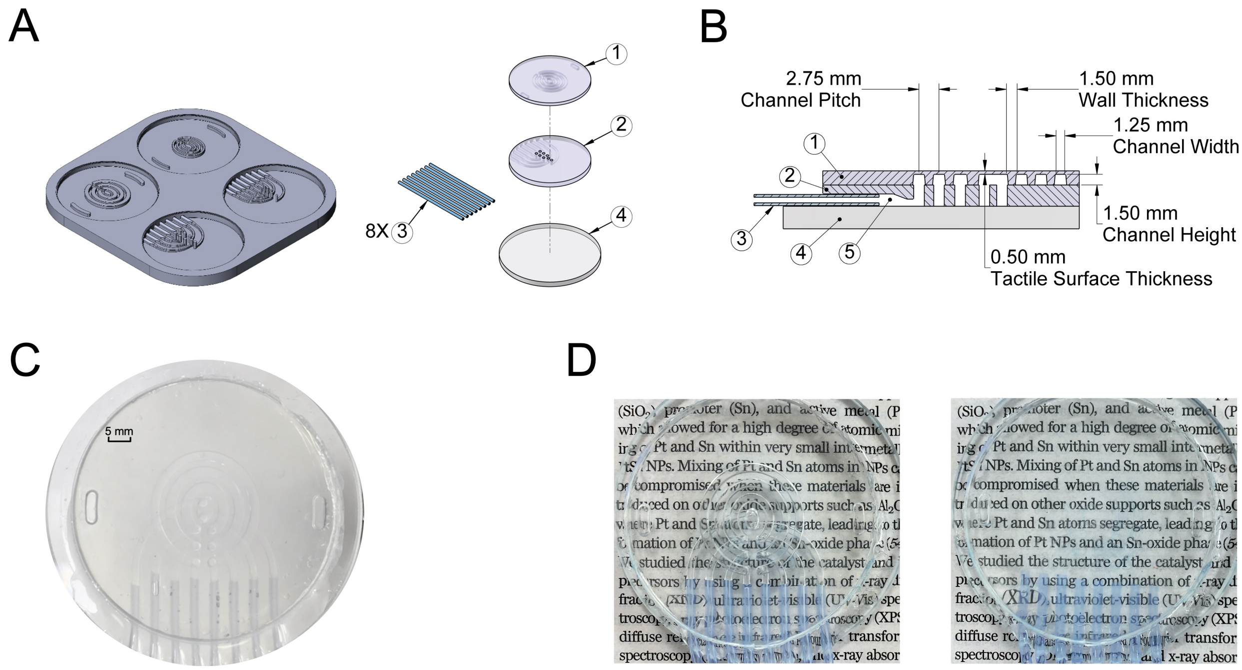

Figure 4.1. Actuator design and fabrication. The multi-channel actuator is comprised of two molded PDMS layers assembled to create four individually addressable discrete activation channels. (**A**)-**left** shows the aluminum mold with two different channel width patterns. The exploded view of (**A**)-**right** and cross-section of (**B**) reveal the channel assembly structure. The molded upper (1) contains 0.5 mm thick by 1.25 mm wide concentric surfaces. These connect by vertical vias to input channels in the molded PDMS lower (2), into which Ø 1.5 mm tubing (3) is inserted for interfacing with the fluidic control system. The actuator then mounts to a borosilicate glass disc (4) and is filled with hydraulic fluid (5). (**C**) Top view of the assembled actuator showing the near transparency of the filled fluid channels. (**D**) The actuator on top of text when the channels filled with air (**left**) and silicone oil (**right**).

Results

Results of actuator mechanical performance

The dual-ended channel design allows for hydraulic priming and independent actuation with no fluidic interference between channels, Fig 4.2A. The vertical displacement of each channel across pressurization levels is measured in Fig 4.2B. Channel 1 produces the largest displacement of 1.2 mm, while channels 2-4 reach displacement of 0.98 mm without over-pressurization. Also, contact force was measured during indentation into the finger pad when the actuator was filled by PG fluid at 0 kPa fluid pressurization (Fig 4.2C) and at 6.9 kPa (Fig 4.2D). The results indicate the actuator can replicate force-displacement characteristics of 33, 45, and 75 kPa solid substrates, by filling channels 1-4 to 0 kPa, channels 1-2 to 6.9 kPa, and channels 1-3 to 6.9 kPa, respectively. Without pressurizing the channels, bulk forces between 0.47 and 0.56 N can be achieved, and when the channels are pressurized at 6.9 kPa, forces between 0.76 to 0.94 N can be achieved.

Results of actuator imaging transparency

The quality of imaging through the actuator was evaluated by spatial variability when indented into a cylindrical surface, Fig 4.3A-C. Measurements of the cylindrical surface obtained upon indentation of the solid substrate at 0, 1.0, and 2.0 mm, exhibit mean square error of 0.0031, 0.0026 and 0.0068 mm, respectively. Comparatively, the filled actuator exhibits higher variability, but still retains low error of 0.0072, 0.0076 and 0.0058 mm. Overall, these results indicate low variability for the filled actuator at indentation depths less than 2 mm.

Results of biomechanical human-subjects experiments

The actuator was indented into the index finger pad at an angle of 30 degrees relative to the finger axis. When filled with air (Fig 4.3D), the observed point clouds are largely scattered due to noise caused by visible channel edges, rendering them unusable (Fig 4.3E). In contrast, when filled with PG fluid, channel edge refractions are much less visible and afford a dense and solid point cloud, Fig 4.3F-G. Fig 4.4A-B shows point clouds generated by 33 and 74 kPa solid substrates and equivalent configurations of the actuator. Nominally, the solid substrates contain a greater number of continuous points than the actuator. From this data, skin cues are generated including contact area, curvature, eccentricity and force. Fig 4.4C-F presents the cues at 0.5 mm increments up to the terminal indentation depth of 2 mm. Comparing the solid substrates and actuator, the growth of the cues is not statistically different (t-test, $p > 0.1$). The cues are however distinct between plots at differing modulus levels as seen when comparing stimuli plots of 33 and 75 kPa. Indeed, it appears that the imaging variance observed in the raw point cloud is less significant once its dimensionality is reduced into skin cues. These results indicate that the actuator simulates similar patterns of skin deformation as the solid substrates.

Results of psychophysical human-subjects experiments

Prior work has found the change rate of contact area of finger pad skin to be highly correlated with our perception of compliance [39]. We compared the change rate of contact area between simulated actuator pairs and evaluate their perceptual discriminability. We created three actuated states to mimic solid substrates with moduli of 33, 45 and 75 kPa. First, we calculated the change rate of contact area by finding the median value from a sequence of change rates at a 0.1 s time interval, Fig 4.5A. When the actuator is more compliant by filling channels 1-4 to 0 kPa, the change rate of contact area (53 mm^2/s) is higher than when channels 1-2 or 1-3 are pressurized to 6.9 kPa (47 and 45 mm^2/s, respectively). Second, from these actuation states, three pairs are formed (45/75, 33/45 and 33/75 kPa) which mimic equivalent solid substrates. The change rate of contact area for each pair is compared in Fig 4.5B, where it is not significantly different between the 45 and 75 kPa pair ($p > 0.05$) but is statistically different between the 33/45 and 33/75 kPa pairs ($p < 0.001$). Third, these distinctions align with psychophysical results in Fig 4.5C, where the participants were not able to perceptually discriminate the 45/75 kPa pair, whereas the 33/75 kPa pair is clearly discriminable, and 33/45 kPa pair is at the 75% threshold.

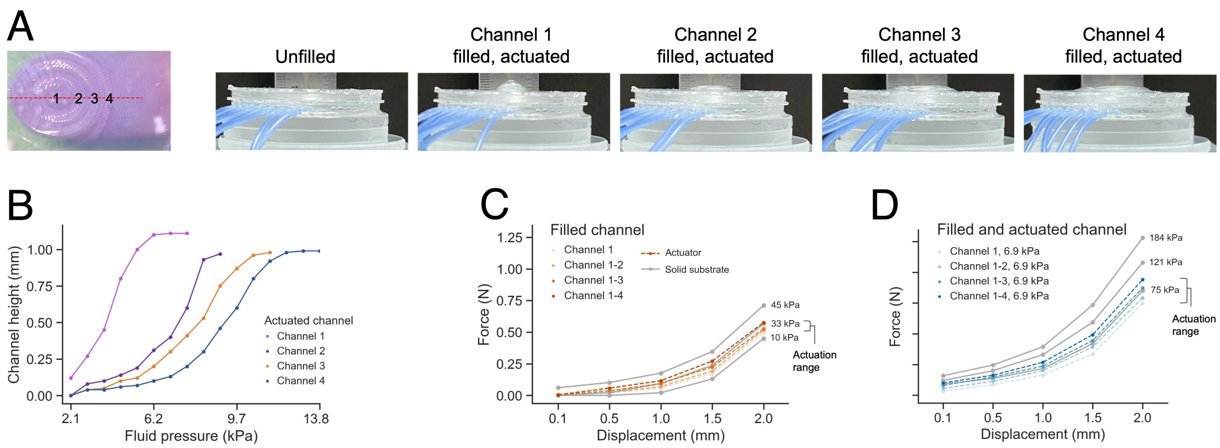

Figure 4.2. Mechanical characterization at fluid pressure and channel selection states. (**A**) Actuator surface displacement when the channels are filled and pressured with PG fluid until the maximum height is reached, before perceived risk of rupture. The channel pressure is assessed by a digital pressure gauge, at a resolution of 0.01 kPa and response time of 0.5 s, and the channel height every 0.69 kPa (0.1 psi). (**B**) The relationship between input fluid pressure and surface height, per channel. (**C**) The force-displacement characteristics of the actuator are evaluated by indentation into the index finger pad at 1.75 mm/s velocity and 2 mm displacement. The contact force generated by filling the channel(s) without actuation is shown in (**C**), while in (**D**) the channels are pressurized to 6.9 kPa after being filled. These measurements are compared to those from solid substrates with known modulus (10-184 kPa).

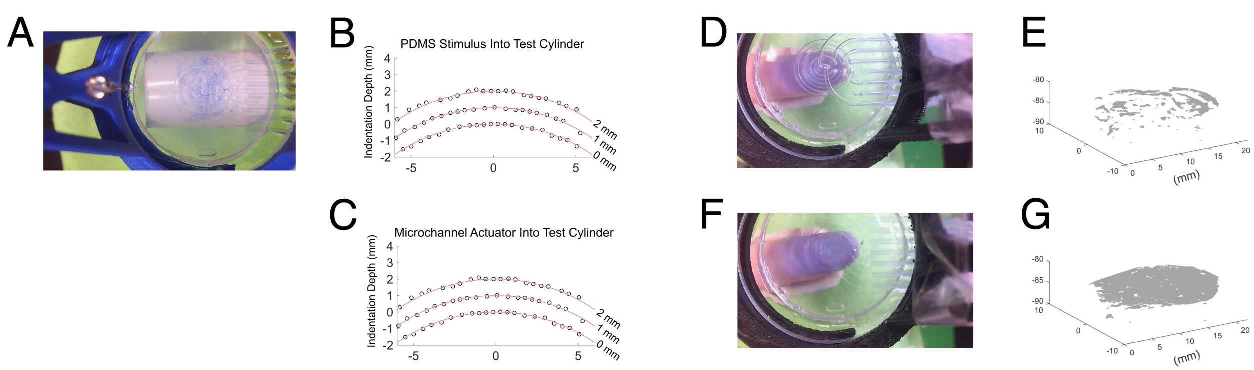

Figure 4.3. Validation of actuator transparency. A 3D imaging system maps surface displacements of a cylinder and index finger pad through actuator. (**A**) Left image of the actuator filled with PG fluid and indented into the cylinder (radius 10.7 mm). (**B**) Surface curvature measurements obtained upon indentation by the 45 kPa solid substrate to 0, 1, and 2 mm, exhibit mean square error of 0.0031, 0.0026 and 0.0068 mm, respectively. (**C**) In comparison, the filled actuator exhibits higher variability, but retains low error of 0.0072, 0.0076 and 0.0058 mm. (**D**) Right image of the actuator filled with ambient pressure air and indented into an index finger pad at angle of 30 degrees, where (**E**) a solid point cloud cannot be formed due to visible channel boundaries. (**F**) Right image of the actuator filled with PG fluid, which qualitatively improves visibility of the underlying finger pad surface, with (**G**) a dense 3D point cloud showing the beneficial effect of PG fluid as a channel filler. Further quantification is performed in Fig 4.4.

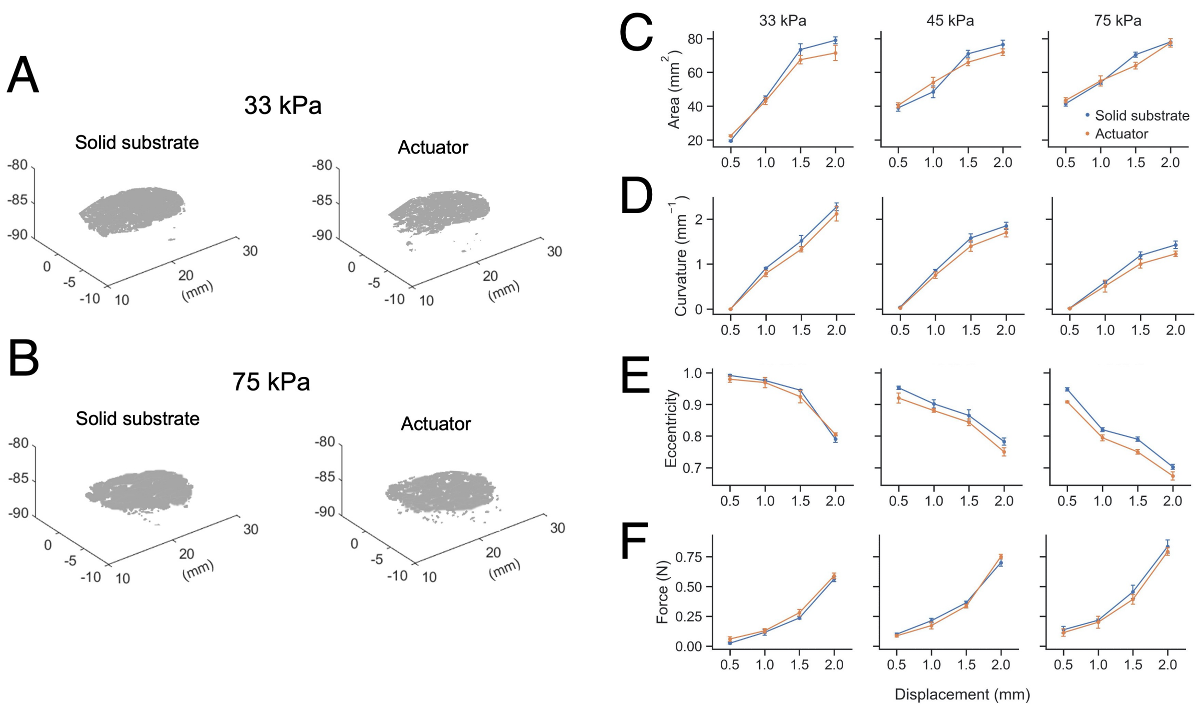

Figure 4.4. Patterns of skin deformation generated by indentation of the actuator and equivalent solid substrates into the index finger pad. (A) 3-D point clouds of skin surface deformation upon indentation with a 33 kPa solid substrate and actuator with channels 1-4 filled to 0 kPa. (B) 3D point clouds for the 75 kPa case, showing a flattening of the finger pad. (C-F) Skin deformation cues of contact area, curvature, eccentricity, and force indicate the actuator and solid substrates produce similar biomechanical results within a plot. Yet these cues are distinct between plots, i.e., at differing modulus levels, e.g., in comparing between 33 and 75 kPa cases.

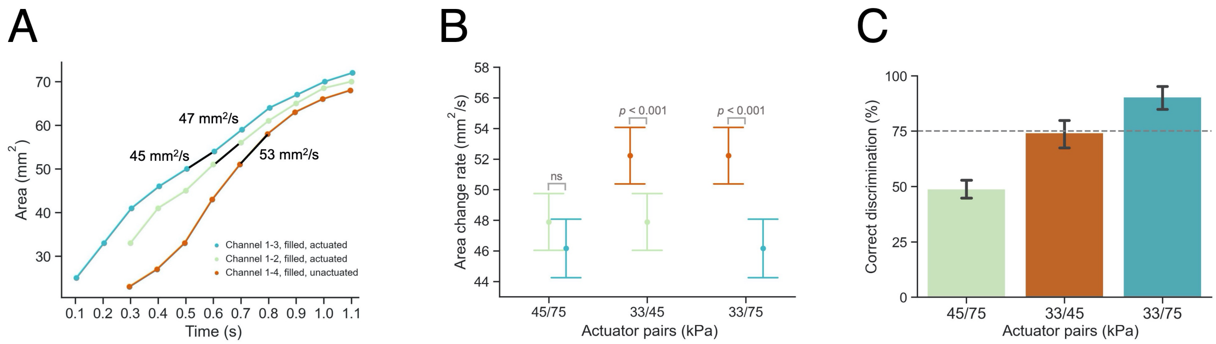

Figure 4.5. Skin deformation cues tied to psychophysical discrimination of actuator pair configurations. Three actuation states are created, equivalent to solid substrates of 33, 45, and 75 kPa modulus, which lead to median change rate of contact area values of 53, 47 and 45 mm^2/s. (**A**) The steps in calculating change rate of contact area from discrete 0.1 s observation points. (**B**) Change rates of contact area for three actuator pairs for all participants aggregated. (**C**) Psychophysical performance in the discrimination task.

Discussion

Soft and compliant actuators under development may soon afford interactions such as touching the hand of another or of tissue in surgery. Though prior works can program states of compliance to regulate contact area and penetration depth, few can directly assess the deformation of the skin surface during actuation. This limits the evaluation of their performance to perceptual judgements. Herein, we developed a transparent, reconfigurable, multi-channel soft actuator through which the deformation of the skin surface can be optically interrogated. This advantage affords a testbed capability to control and replay cutaneous cues that may correlate with our percept of compliance. Moreover, the actuator achieves a greater dynamic range of surface displacement and contact force compared to other transparent soft actuators.

Prior programmable devices have altered percepts of compliance by varying magnitudes of external force over the spatial extent of the skin surface [23], [114]. Compared to devices that optimize the positioning of rigid surfaces [95]–[98], [117], the aforementioned actuators with compliant and conformable surfaces conform to the shape of the finger and its geometry, and onset less abruptly at forces of millinewtons. Most soft actuators are not transparent, however, and those which have been limited in their deliverable force range. To successfully perceive compliance, forces at the index finger should span a dynamic range of about 33 to 1480 mN [118], [119]. In comparison, transparent actuators generate forces of 255-300 mN and displacements of 500-600 μm [24], [32]. Although not used in with imaging, Frediani et al. used pneumatic and electrical actuation of an elastomer chamber to achieve forces of 1 N and displacements of 3.5 mm [23], [103]. In comparison, the actuator described herein provides contact forces of 1 N and vertical displacements of 1.2 mm. Unlike such prior devices with a single actuation chamber, the actuator herein affords four programmable channels to modulate the force and spatial extent of the skin surface, where each channel can be pressurized independently. To fully decipher the cutaneous cues that drive perception, we need to be able to control and replay, not just observe, the skin's surface deformation while concurrently evaluating a person's perceptual response. The optical transparency of the actuator herein provides the capability to directly observe such dynamics at various configurations of compliance. We demonstrate its configuration to three states of compliance, derived from direct observations of skin cues, which leads to perceptual discrimination spanning chance performance, the 75% threshold, and near 100% performance. Additional work is needed to define the optimal density, dimensions, and geometric patterning of the channels to best reproduce cutaneous cues tied to contact area and force that we observe with solid substrates [4]–[6], [39], [51], [55], [116]. Another next step is to dynamically actuate the channels while in contact with the skin surface to afford active touch, and understand how fast the skin needs to move with dynamically changing stimuli and human interactions.

Overall conclusions and future work

In this dissertation, we performed significant groundwork towards understanding the correlations between skin deformation and tactile perception of material compliance. The overall objective of this work was to encode and manipulate the optimal skin cues that optimally drive distinct percepts of compliance across and within individuals. We sought to address this goal by first deriving meaningful spatiotemporal cues to characterize skin deformation through 3-D imaging techniques, coupled with biomechanical and psychophysical experimentation for evaluating their associations with perceptual responses. Then we investigated the factors of indentation velocity, depth and time duration, and we found those factors are significantly influential in the evolvement of skin deformation as well as in the perceptual discriminability. Second, we studied differences in skin properties across individuals and found those differences influence individuals' discrimination performance. We evaluated the relationships among skin properties including finger size, stiffness and fingertip ridge breadth, and found that skin stiffness, which was highly correlated with finger size, played a dominate role in driving perception of compliance. We further decoupled the effects of finger stiffness and size on tactile percepts by modulating the participants' skin stiffness alone, and the results indicate that an individual's discriminability can be largely improved by reducing skin stiffness. Moreover, by using machine learning algorithms and statistical modeling, we discovered two distinct groups within a cohort of young population, with differences in both skin properties and perceptual discriminability. Consequently, predictive models were built to anticipant people's discrimination performance based on their skin properties. Finally, to move from scientific theory to tangible practices, we designed a transparent hydraulic actuator to modulate skin deformation that delivers distinct percepts of compliance. By incorporating the actuator with the imaging system, we are able to directly access visualization of contact surface during actuation. In doing so, we developed a close-loop system that simultaneously generates tactile sensations with direct visual access of skin dynamics.

There are two main perspectives which those insights developed in this dissertation can benefit in. The first perspective is in haptic science. First, we can extend our findings from

Aim 2 to active touch, to evaluate if we can modulate people's tactile discriminability by manipulating their finger properties. Second, by using the clear actuator designed in Aim 3 which provides direct visualization of contact surface, we can revisit existing results in the literature about the way skin deforms and how it relates to human tactile perception. We can improve the spatial and temporal resolution of the actuator using more precise printing and molding technologies, which can afford a wider range of reconfigurations of surface pattern. With more controlled skin deformation, we can directly validate the usefulness of skin cues and also generate naturalistic and effective tactile sensations. Furthermore, as currently we evaluate the actuator's performance in static states due to the limitation of imaging capability, we can design the experiment in a dynamic manner by breaking up the time duration of contact into discrete time intervals so that we can access the information about intermediate changes throughout indentation. Moreover, we can introduce dynamic control of the actuator by incorporating it with a syringe pumping system in which each channel can be activated with controlled speed and magnitude. In doing so, we can directly manipulate the change rate of skin cues, i.e., contact area and eccentricity change rates, to stimulate distinct perceptions. The second perspective is in haptic engineering. First, the clear actuator paved a way of developing close-loop systems for tactile devices. Since most of the haptic devices do not have access of information about skin deformation during interaction, they cannot test and evaluate the input and output of the system. On the other hand, the clear actuator provides the capability of evaluating the input, which is the generated skin deformation cues, as well as the output of the system, which is the psychophysical responses. Additionally, for the community in human-computer interface (HCI), we can design new patterns that use predictive models we developed in Aim 2 to optimize user experiences.

Publications

Accepted works

Journal Papers

[1] **B. Li,** S. C. Hauser, and G. J. Gerling, “Faster indentation influences skin deformation to reduce tactile discriminability of compliant objects,” IEEE Transactions on Haptics, pp. 1–11, 2023

Conference Papers (Peer-reviewed publications)

[1] **B. Li**, S. Hauser, and G. J. Gerling, “Identifying 3-D spatiotemporal skin deformation cues evoked in interacting with compliant elastic surfaces,” in 2020 IEEE Haptics Symposium (HAPTICS), Mar. 2020, pp. 35–40.

[2] **B. Li** and G. J. Gerling, “Individual differences impacting skin deformation and tactile discrimination with compliant elastic surfaces,” in 2021 IEEE World Haptics Conference (WHC), Jul. 2021, pp. 721–726.

W.I.P (short) Conference Papers

[1] **B. Li**, J. Lee, and G. J. Gerling, “A Magnetorheological Elastomer Device for Programmable Actuation and Sensing of Soft Haptic Experiences,” in 2021 IEEE World Haptics Conference (WHC), Jul. 2021, pp. 349–349.

In progress works

Journal Papers

[1] **B. Li** and G. J. Gerling, “An individual’s skin stiffness predicts their tactile acuity,” in writing, to be submitted to *Proceedings of the National Academy of Sciences,2023.*

[2] **B. Li,** A. R. Sharpe and G. J. Gerling, “A transparent and reconfigurable hydraulic actuator to visualize the finger pad surface at distinct percepts of compliance,” in preparation.

Conference Papers

[1] **B. Li**, J. Lee and G. J. Gerling, “Perceptibility of programmable softness displays using magnetorheological elastomers,” under review, *Human Factors and Ergonomics Society 67th International Annual Meeting Conference, 2023.*

Reference

[1] C. Xu, Y. Wang, and G. J. Gerling, “An elasticity-curvature illusion decouples cutaneous and proprioceptive cues in active exploration of soft objects,” *PLOS Computational Biology*, vol. 17, no. 3, p. e1008848, Mar. 2021, doi: 10.1371/journal.pcbi.1008848.

[2] K. Johnson, “Closing in on the neural mechanisms of finger joint angle sense. Focus on ‘Quantitative analysis of dynamic strain sensitivity in human skin mechanoreceptors,’” *J. Neurophysiol.*, vol. 92, no. 6, pp. 3167–3168, Dec. 2004.

[3] B. B. Edin, “lamotte_softness_2000,” *J Neurophysiol*, vol. 67, no. 5, pp. 1105–1113, May 1992, doi: 10.1152/jn.1992.67.5.1105.

[4] G. Ambrosi, A. Bicchi, D. De Rossi, and E. P. Scilingo, “The role of contact area spread rate in haptic discrimination of softness,” in *Proceedings 1999 IEEE International Conference on Robotics and Automation (Cat. No.99CH36288C)*, May 1999, vol. 1, pp. 305–310 vol.1. doi: 10.1109/ROBOT.1999.769996.

[5] A. Moscatelli *et al.*, “The Change in Fingertip Contact Area as a Novel Proprioceptive Cue,” *Current Biology*, vol. 26, no. 9, pp. 1159–1163, May 2016, doi: 10.1016/j.cub.2016.02.052.

[6] C. Dhong *et al.*, “Role of indentation depth and contact area on human perception of softness for haptic interfaces,” *Sci Adv*, vol. 5, no. 8, p. eaaw8845, Aug. 2019, doi: 10.1126/sciadv.aaw8845.

[7] M. Di Luca, B. Knörlein, M. O. Ernst, and M. Harders, “Effects of visual-haptic asynchronies and loading-unloading movements on compliance perception,” *Brain Res Bull*, vol. 85, no. 5, pp. 245–259, Jun. 2011, doi: 10.1016/j.brainresbull.2010.02.009.

[8] M. Liu, A. Batista, S. Bensmaia, and D. J. Weber, “Information about contact force and surface texture is mixed in the firing rates of cutaneous afferent neurons,” *Journal of Neurophysiology*, vol. 125, no. 2, pp. 496–508, Feb. 2021, doi: 10.1152/jn.00725.2019.

[9] C. Schuermann, R. Haschke, and H. Ritter, “Modular high speed tactile sensor system with video interface,” Jan. 2009.

[10] M. A. Srinivasan and R. H. LaMotte, “Tactual discrimination of softness,” *Journal of Neurophysiology*, vol. 73, no. 1, Art. no. 1, 1995.

[11] S. C. Hauser and G. J. Gerling, “Force-rate Cues Reduce Object Deformation Necessary to Discriminate Compliances Harder than the Skin,” *IEEE Transactions on Haptics*, vol. 11, no. 2, pp. 232–240, Apr. 2018, doi: 10.1109/TOH.2017.2715845.

[12] B. M. Dzidek, M. J. Adams, J. W. Andrews, Z. Zhang, and S. A. Johnson, “Contact mechanics of the human finger pad under compressive loads,” *J. R. Soc. Interface.*, vol. 14, no. 127, p. 20160935, Feb. 2017, doi: 10.1098/rsif.2016.0935.

[13] A. Barrea, B. P. Delhaye, P. Lefèvre, and J.-L. Thonnard, “Perception of partial slips under tangential loading of the fingertip,” *Sci Rep*, vol. 8, no. 1, p. 7032, May 2018, doi: 10.1038/s41598-018-25226-w.

[14] H. Khamis *et al.*, "Friction sensing mechanisms for perception and motor control: passive touch without sliding may not provide perceivable frictional information," *Journal of Neurophysiology*, vol. 125, no. 3, pp. 809–823, Mar. 2021, doi: 10.1152/jn.00504.2020.

[15] M. A. Srinivasan, J. M. Whitehouse, and R. H. LaMotte, "Tactile detection of slip: surface microgeometry and peripheral neural codes," *Journal of Neurophysiology*, vol. 63, no. 6, pp. 1323–1332, Jun. 1990, doi: 10.1152/jn.1990.63.6.1323.

[16] S. M. Kolly, R. Wattenhofer, and S. Welten, "A personal touch: recognizing users based on touch screen behavior," in *Proceedings of the Third International Workshop on Sensing Applications on Mobile Phones*, New York, NY, USA, Nov. 2012, pp. 1–5. doi: 10.1145/2389148.2389149.

[17] D. Olczak, V. Sukumar, and J. A. Pruszynski, "Edge orientation perception during active touch," *Journal of Neurophysiology*, vol. 120, no. 5, pp. 2423–2429, Nov. 2018, doi: 10.1152/jn.00280.2018.

[18] R. M. Peters, E. Hackeman, and D. Goldreich, "Diminutive Digits Discern Delicate Details: Fingertip Size and the Sex Difference in Tactile Spatial Acuity," *J Neurosci*, vol. 29, no. 50, pp. 15756–15761, Dec. 2009, doi: 10.1523/JNEUROSCI.3684-09.2009.

[19] B. Pleger *et al.*, "A complementary role of intracortical inhibition in age-related tactile degradation and its remodelling in humans," *Scientific Reports*, vol. 6, no. 1, Art. no. 1, Jun. 2016, doi: 10.1038/srep27388.

[20] K. L. Woodward, "The Relationship between Skin Compliance, Age, Gender, and Tactile Discriminative Thresholds in Humans," *Somatosensory & Motor Research*, vol. 10, no. 1, pp. 63–67, Jan. 1993, doi: 10.3109/08990229309028824.

[21] F. Vega-Bermudez and K. O. Johnson, "Fingertip skin conformance accounts, in part, for differences in tactile spatial acuity in young subjects, but not for the decline in spatial acuity with aging," *Perception & Psychophysics*, vol. 66, no. 1, pp. 60–67, Jan. 2004, doi: 10.3758/BF03194861.

[22] T. Hamasaki, T. Yamaguchi, and M. Iwamoto, "Estimating the influence of age-related changes in skin stiffness on tactile perception for static stimulations," *Journal of Biomechanical Science and Engineering*, vol. advpub, 2018, doi: 10.1299/jbse.17-00575.

[23] G. Frediani, H. Boys, M. Ghilardi, S. Poslad, J. J. C. Busfield, and F. Carpi, "A Soft Touch: Wearable Tactile Display of Softness Made of Electroactive Elastomers," *Advanced Materials Technologies*, vol. n/a, no. n/a, p. 2100016, doi: https://doi.org/10.1002/admt.202100016.

[24] E. Leroy, R. Hinchet, and H. Shea, "Multimode Hydraulically Amplified Electrostatic Actuators for Wearable Haptics," *Advanced Materials*, vol. 32, no. 36, p. 2002564, 2020, doi: 10.1002/adma.202002564.

[25] Y.-L. Park and R. J. Wood, "Smart pneumatic artificial muscle actuator with embedded microfluidic sensing," in *2013 IEEE SENSORS*, Nov. 2013, pp. 1–4. doi: 10.1109/ICSENS.2013.6688298.

[26] A. Talhan and S. Jeon, “Pneumatic Actuation in Haptic-Enabled Medical Simulators: A Review,” *IEEE Access*, vol. 6, pp. 3184–3200, 2018, doi: 10.1109/ACCESS.2017.2787601.

[27] G. Reardon *et al.*, “Cutaneous Wave Propagation Shapes Tactile Motion: Evidence from Air-Coupled Ultrasound,” in *2019 IEEE World Haptics Conference (WHC)*, Jul. 2019, pp. 628–633. doi: 10.1109/WHC.2019.8816150.

[28] J. Lee and G. Lee, “Designing a Non-contact Wearable Tactile Display Using Airflows,” in *Proceedings of the 29th Annual Symposium on User Interface Software and Technology*, New York, NY, USA, Oct. 2016, pp. 183–194. doi: 10.1145/2984511.2984583.

[29] T.-H. Yang *et al.*, “Development of a miniature tunable stiffness display using MR fluids for haptic application,” *Sensors and Actuators A: Physical*, vol. 163, no. 1, pp. 180–190, Sep. 2010, doi: 10.1016/j.sna.2010.07.004.

[30] M. Cavdan, K. Doerschner, and K. Drewing, “Task and material properties interactively affect softness explorations along different dimensions,” *IEEE Transactions on Haptics*, pp. 1–1, 2021, doi: 10.1109/TOH.2021.3069626.

[31] C. Xu, H. He, S. C. Hauser, and G. J. Gerling, “Tactile Exploration Strategies With Natural Compliant Objects Elicit Virtual Stiffness Cues,” *IEEE Transactions on Haptics*, vol. 13, no. 1, pp. 4–10, Jan. 2020, doi: 10.1109/TOH.2019.2959767.

[32] S. Mun *et al.*, “Electro-Active Polymer Based Soft Tactile Interface for Wearable Devices,” *IEEE Transactions on Haptics*, vol. 11, no. 1, pp. 15–21, Jan. 2018, doi: 10.1109/TOH.2018.2805901.

[33] I. Poupyrev and S. Maruyama, “Tactile interfaces for small touch screens,” in *Proceedings of the 16th annual ACM symposium on User interface software and technology*, New York, NY, USA, Nov. 2003, pp. 217–220. doi: 10.1145/964696.964721.

[34] M. C. Lin and M. A. Otaduy, *Haptic rendering: Foundations, algorithms, and applications*. 2008.

[35] M. A. Srinivasan and R. H. LaMotte, “Tactual discrimination of softness: abilities and mechanisms,” in *Somesthesis and the Neurobiology of the Somatosensory Cortex*, P. O. Franzén, P. R. Johansson, and P. L. Terenius, Eds. Birkhäuser Basel, 1996, pp. 123–135. doi: 10.1007/978-3-0348-9016-8_11.

[36] W. M. Bergmann Tiest and A. M. Kappers, “Cues for haptic perception of compliance,” *Haptics, IEEE Transactions on*, vol. 2, no. 4, Art. no. 4, 2009.

[37] C. Xu, Y. Wang, and G. J. Gerling, “An elasticity-curvature illusion decouples cutaneous and proprioceptive cues in active exploration of soft objects,” *PLOS Computational Biology*, vol. 17, no. 3, p. e1008848, Mar. 2021, doi: 10.1371/journal.pcbi.1008848.

[38] I. Birznieks, V. G. Macefield, G. Westling, and R. S. Johansson, “Slowly Adapting Mechanoreceptors in the Borders of the Human Fingernail Encode Fingertip Forces,” *J. Neurosci.*, vol. 29, no. 29, pp. 9370–9379, Jul. 2009, doi: 10.1523/JNEUROSCI.0143-09.2009.

[39] B. Li and G. J. Gerling, “Individual differences impacting skin deformation and tactile discrimination with compliant elastic surfaces,” in *2021 IEEE World Haptics Conference (WHC)*, Jul. 2021, pp. 721–726. doi: 10.1109/WHC49131.2021.9517222.

[40] W. M. Bergmann Tiest and A. M. Kappers, “Physical Aspects of Softness Perception,” in *Multisensory Softness*, Springer London, 2014, pp. 3–15. Accessed: Jan. 19, 2017. [Online]. Available: http://link.springer.com/chapter/10.1007/978-1-4471-6533-0_1

[41] A. Bicchi, E. P. Scilingo, and D. De Rossi, “Haptic discrimination of softness in teleoperation: the role of the contact area spread rate,” *IEEE Transactions on Robotics and Automation*, vol. 16, no. 5, pp. 496–504, Oct. 2000, doi: 10.1109/70.880800.

[42] W. Chen, H. Khamis, I. Birznieks, N. F. Lepora, and S. J. Redmond, “Tactile Sensors for Friction Estimation and Incipient Slip Detection—Toward Dexterous Robotic Manipulation: A Review,” *IEEE Sensors Journal*, vol. 18, no. 22, pp. 9049–9064, Nov. 2018, doi: 10.1109/JSEN.2018.2868340.

[43] R. A. Romeo, C. M. Oddo, M. C. Carrozza, E. Guglielmelli, and L. Zollo, “Slippage Detection with Piezoresistive Tactile Sensors,” *Sensors (Basel)*, vol. 17, no. 8, p. 1844, Aug. 2017, doi: 10.3390/s17081844.

[44] W. R. Provancher and N. D. Sylvester, “Fingerpad Skin Stretch Increases the Perception of Virtual Friction,” *IEEE Transactions on Haptics*, vol. 2, no. 4, pp. 212–223, Oct. 2009, doi: 10.1109/TOH.2009.34.

[45] Z. F. Quek, S. B. Schorr, I. Nisky, A. M. Okamura, and W. R. Provancher, “Sensory augmentation of stiffness using fingerpad skin stretch,” in *2013 World Haptics Conference (WHC)*, Apr. 2013, pp. 467–472. doi: 10.1109/WHC.2013.6548453.

[46] Y. Wang, K. L. Marshall, Y. Baba, E. A. Lumpkin, and G. J. Gerling, “Compressive Viscoelasticity of Freshly Excised Mouse Skin Is Dependent on Specimen Thickness, Strain Level and Rate,” *PLOS ONE*, vol. 10, no. 3, p. e0120897, Mar. 2015, doi: 10.1371/journal.pone.0120897.

[47] R. LaMotte and M. Srinivasan, “Tactile discrimination of shape: responses of rapidly adapting mechanoreceptive afferents to a step stroked across the monkey fingerpad,” *J. Neurosci.*, vol. 7, no. 6, pp. 1672–1681, Jun. 1987, doi: 10.1523/JNEUROSCI.07-06-01672.1987.

[48] D. A. Poulos *et al.*, “The Neural Signal for the Intensity of a Tactile Stimulus,” *J. Neurosci.*, vol. 4, no. 8, pp. 2016–2024, 1984.

[49] S. Simonetti, K. Dahl, and C. Krarup, “Different indentation velocities activate different populations of mechanoreceptors in humans,” *Muscle & Nerve*, vol. 21, no. 7, pp. 858–868, 1998, doi: 10.1002/(SICI)1097-4598(199807)21:7<858::AID-MUS3>3.0.CO;2-5.

[50] S. C. Hauser and G. J. Gerling, “Imaging the 3-D deformation of the finger pad when interacting with compliant materials,” in *IEEE Haptics Symposium, HAPTICS*, May 2018, vol. 2018-March, pp. 7–13. doi: 10.1109/HAPTICS.2018.8357145.

[51] B. Li, S. Hauser, and G. J. Gerling, “Identifying 3-D spatiotemporal skin deformation cues evoked in interacting with compliant elastic surfaces,” in *2020 IEEE Haptics Symposium (HAPTICS)*, Mar. 2020, pp. 35–40. doi: 10.1109/HAPTICS45997.2020.ras.HAP20.22.5a9b38d8.

[52] E. Miguel *et al.*, “Characterization of nonlinear finger pad mechanics for tactile rendering,” in *IEEE World Haptics Conference, WHC 2015*, 2015. doi: 10.1109/WHC.2015.7177692.

[53] G. J. Gerling, S. C. Hauser, B. R. Soltis, A. K. Bowen, K. D. Fanta, and Y. Wang, “A Standard Methodology to Characterize the Intrinsic Material Properties of Compliant Test Stimuli,” *IEEE Transactions on Haptics*, vol. 11, no. 4, pp. 498–508, Oct. 2018, doi: 10.1109/TOH.2018.2825396.

[54] S. C. Hauser and G. J. Gerling, “Measuring tactile cues at the fingerpad for object compliances harder and softer than the skin,” in *2016 IEEE Haptics Symposium (HAPTICS)*, Apr. 2016, pp. 247–252. doi: 10.1109/HAPTICS.2016.7463185.

[55] C. Xu and G. J. Gerling, “Time-dependent Cues Encode the Minimum Exploration Time in Discriminating Naturalistic Compliances,” in *2020 IEEE Haptics Symposium (HAPTICS)*, Mar. 2020, pp. 22–27. doi: 10.1109/HAPTICS45997.2020.ras.HAP20.7.ec43f6a7.

[56] A. Metzger and K. Drewing, “Effects of Stimulus Exploration Length and Time on the Integration of Information in Haptic Softness Discrimination,” *IEEE Transactions on Haptics*, vol. 12, no. 4, pp. 451–460, Oct. 2019, doi: 10.1109/TOH.2019.2899298.

[57] A. Metzger, A. Lezkan, and K. Drewing, “Integration of serial sensory information in haptic perception of softness,” *Journal of Experimental Psychology: Human Perception and Performance*, vol. 44, no. 4, pp. 551–565, 2018, doi: 10.1037/xhp0000466.

[58] H. Z. Tan, N. I. Durlach, G. L. Beauregard, and M. A. Srinivasan, “Manual discrimination of compliance using active pinch grasp: the roles of force and work cues,” *Percept Psychophys*, vol. 57, no. 4, pp. 495–510, May 1995, doi: 10.3758/bf03213075.

[59] L. Kaim and K. Drewing, “Exploratory Strategies in Haptic Softness Discrimination Are Tuned to Achieve High Levels of Task Performance,” *IEEE Transactions on Haptics*, vol. 4, no. 4, pp. 242–252, Oct. 2011, doi: 10.1109/TOH.2011.19.

[60] L. Willemet, K. Kanzari, J. Monnoyer, I. Birznieks, and M. Wiertlewski, “Initial contact shapes the perception of friction,” *Proceedings of the National Academy of Sciences*, vol. 118, no. 49, p. e2109109118, Dec. 2021, doi: 10.1073/pnas.2109109118.

[61] M. Tomimoto, “The frictional pattern of tactile sensations in anthropomorphic fingertip,” *Tribology International*, vol. 44, no. 11, pp. 1340–1347, Oct. 2011, doi: 10.1016/j.triboint.2010.12.004.

[62] T. Maeno, K. Kobayashi, and N. Yamazaki, “Relationship between the Structure of Human Finger Tissue and the Location of Tactile Receptors,” *JSME International Journal Series C*, vol. 41, no. 1, pp. 94–100, 1998, doi: 10.1299/jsmec.41.94.

[63] J. C. Stevens and K. K. Choo, “Spatial Acuity of the Body Surface over the Life Span,” *Somatosensory & Motor Research*, vol. 13, no. 2, pp. 153–166, Jan. 1996, doi: 10.3109/08990229609051403.

[64] J. C. Stevens and M. Q. Patterson, “Dimensions of Spatial Acuity in the Touch Sense: Changes over the Life Span,” *Somatosensory & Motor Research*, vol. 12, no. 1, pp. 29–47, Jan. 1995, doi: 10.3109/08990229509063140.

[65] W. Montagna and K. Carlisle, “Structural changes in aging human skin,” *J Invest Dermatol*, vol. 73, no. 1, pp. 47–53, Jul. 1979, doi: 10.1111/1523-1747.ep12532761.

[66] G. A. Gescheider, S. J. Bolanowski, K. L. Hall, K. E. Hoffman, and R. T. Verrillo, “The Effects of Aging on Information-Processing Channels in the Sense of Touch: I. Absolute Sensitivity,” *Somatosensory & Motor Research*, vol. 11, no. 4, pp. 345–357, Jan. 1994, doi: 10.3109/08990229409028878.

[67] R. M. Peters and D. Goldreich, “Tactile Spatial Acuity in Childhood: Effects of Age and Fingertip Size,” *PLOS ONE*, vol. 8, no. 12, p. e84650, Dec. 2013, doi: 10.1371/journal.pone.0084650.

[68] A. Abdouni, G. Moreau, R. Vargiolu, and H. Zahouani, “Static and active tactile perception and touch anisotropy: aging and gender effect,” *Scientific Reports*, vol. 8, no. 1, Art. no. 1, Sep. 2018, doi: 10.1038/s41598-018-32724-4.

[69] J. L. Bowden and P. A. McNulty, “Age-related changes in cutaneous sensation in the healthy human hand,” *AGE*, vol. 35, no. 4, pp. 1077–1089, Aug. 2013, doi: 10.1007/s11357-012-9429-3.

[70] M. M. Wickremaratchi and J. G. Llewelyn, “Effects of ageing on touch,” *Postgraduate Medical Journal*, vol. 82, no. 967, pp. 301–304, May 2006, doi: 10.1136/pgmj.2005.039651.

[71] A. Abdouni, M. Djaghloul, C. Thieulin, R. Vargiolu, C. Pailler-Mattei, and H. Zahouani, “Biophysical properties of the human finger for touch comprehension: influences of ageing and gender,” *Royal Society Open Science*, vol. 4, no. 8, p. 170321, doi: 10.1098/rsos.170321.

[72] G. O. Gibson and J. C. Craig, “The effect of force and conformance on tactile intensive and spatial sensitivity,” *Exp Brain Res*, vol. 170, no. 2, pp. 172–181, Apr. 2006, doi: 10.1007/s00221-005-0200-1.

[73] “Tactile spatial resolution. II. Neural representation of Bars, edges, and gratings in monkey primary afferents | Journal of Neurophysiology.” https://journals.physiology.org/doi/abs/10.1152/jn.1981.46.6.1192 (accessed Jul. 30, 2022).

[74] K. M. Hudson *et al.*, “Effects of changing skin mechanics on the differential sensitivity to surface compliance by tactile afferents in the human finger pad,” *Journal of Neurophysiology*, vol. 114, no. 4, pp. 2249–2257, Oct. 2015, doi: 10.1152/jn.00176.2014.

[75] Y. K. Dillon, J. Haynes, and M. Henneberg, “The relationship of the number of Meissner’s corpuscles to dermatoglyphic characters and finger size,” *J Anat*, vol. 199, no. Pt 5, pp. 577–584, Nov. 2001, doi: 10.1046/j.1469-7580.2001.19950577.x.

[76] D. Z. Loesch and N. G. Martin, "Finger ridge patterns and tactile sensitivity," *Annals of Human Biology*, vol. 11, no. 2, pp. 113–124, Jan. 1984, doi: 10.1080/03014468400006961.

[77] D. Z. Loesch and N. G. Martin, "Relationships between minute characteristics of finger ridges and pattern size and shape," *Annals of Human Biology*, vol. 11, no. 2, pp. 125–132, Jan. 1984, doi: 10.1080/03014468400006971.

[78] G. J. Gerling and G. W. Thomas, "Fingerprint lines may not directly affect SA-I mechanoreceptor response," *Somatosensory & Motor Research*, vol. 25, no. 1, Art. no. 1, Jan. 2008, doi: 10.1080/08990220701838996.

[79] G. J. Gerling, "SA-I Mechanoreceptor Position in Fingertip Skin May Impact Sensitivity to Edge Stimuli," *Applied Bionics and Biomechanics*, vol. 7, no. 1, pp. 19–29, 2010, doi: 10.1080/11762320903069992.

[80] E. Miguel *et al.*, "Characterization of nonlinear finger pad mechanics for tactile rendering," in *2015 IEEE World Haptics Conference (WHC)*, Jun. 2015, pp. 63–68. doi: 10.1109/WHC.2015.7177692.

[81] C. Oprişan, V. Cârlescu, A. Barnea, G. Prisacaru, D. N. Olaru, and G. Plesu, "Experimental determination of the Young's modulus for the fingers with application in prehension systems for small cylindrical objects," *IOP Conf. Ser.: Mater. Sci. Eng.*, vol. 147, p. 012058, Aug. 2016, doi: 10.1088/1757-899X/147/1/012058.

[82] Hyun-Yong Han and S. Kawamura, "Analysis of stiffness of human fingertip and comparison with artificial fingers," in *IEEE SMC'99 Conference Proceedings. 1999 IEEE International Conference on Systems, Man, and Cybernetics (Cat. No.99CH37028)*, Oct. 1999, vol. 2, pp. 800–805 vol.2. doi: 10.1109/ICSMC.1999.825364.

[83] A. Z. Mundorff, E. J. Bartelink, and T. A. Murad, "Sexual Dimorphism in Finger Ridge Breadth Measurements: A Tool for Sex Estimation from Fingerprints," *Journal of Forensic Sciences*, vol. 59, no. 4, pp. 891–897, 2014, doi: 10.1111/1556-4029.12449.

[84] A. R. Tilley, "HENRY DREYfUSS ASSOCIATES," p. 97.

[85] M. A. Srinivasan and R. H. LaMotte, "Tactual discrimination of softness," *Journal of Neurophysiology*, vol. 73, no. 1, Art. no. 1, 1995.

[86] B. Li, S. C. Hauser, and G. J. Gerling, "Faster indentation influences skin deformation to reduce tactile discriminability of compliant objects," IEEE Transactions on Haptics.

[87] G. Serhat, Y. Vardar, and K. J. Kuchenbecker, "Contact evolution of dry and hydrated fingertips at initial touch," *PLoS ONE*, vol. 17, no. 7, p. e0269722, Jul. 2022, doi: 10.1371/journal.pone.0269722.

[88] M. Nuszbaum, A. Voss, K. C. Klauer, and T. Betsch, "Assessing Individual Differences in the Use of Haptic Information Using a German Translation of the Need for Touch Scale," *Social Psychology*, vol. 41, no. 4, pp. 263–274, Jan. 2010, doi: 10.1027/1864-9335/a000035.

[89] J. Peck and T. L. Childers, “Individual Differences in Haptic Information Processing: The ‘Need for Touch’ Scale,” *Journal of Consumer Research*, vol. 30, no. 3, pp. 430–442, Dec. 2003, doi: 10.1086/378619.

[90] A. V. Citrin, D. E. Stem, E. R. Spangenberg, and M. J. Clark, “Consumer need for tactile input,” *Journal of Business Research*, vol. 56, no. 11, pp. 915–922, Nov. 2003, doi: 10.1016/S0148-2963(01)00278-8.

[91] J. Peck and J. Wiggins, “It Just Feels Good: Customers’ Affective Response to Touch and Its Influence on Persuasion,” *Journal of Marketing*, vol. 70, no. 4, pp. 56–69, Oct. 2006, doi: 10.1509/jmkg.70.4.056.

[92] G. J. Broussard *et al.*, “In vivo measurement of afferent activity with axon-specific calcium imaging,” *Nat Neurosci*, vol. 21, no. 9, Art. no. 9, Sep. 2018, doi: 10.1038/s41593-018-0211-4.

[93] X. Hernot, O. Bartier, Y. Bekouche, R. El Abdi, and G. Mauvoisin, “Influence of penetration depth and mechanical properties on contact radius determination for spherical indentation,” *International Journal of Solids and Structures*, vol. 43, no. 14, pp. 4136–4153, Jul. 2006, doi: 10.1016/j.ijsolstr.2005.06.007.

[94] M. Farajian, R. Leib, H. Kossowsky, T. Zaidenberg, F. A. Mussa-Ivaldi, and I. Nisky, “Stretching the skin immediately enhances perceived stiffness and gradually enhances the predictive control of grip force,” *eLife*, vol. 9, p. e52653, Apr. 2020, doi: 10.7554/eLife.52653.

[95] H. Kim, H. Yi, H. Lee, and W. Lee, “HapCube: A Wearable Tactile Device to Provide Tangential and Normal Pseudo-Force Feedback on a Fingertip,” in *Proceedings of the 2018 CHI Conference on Human Factors in Computing Systems*, New York, NY, USA: Association for Computing Machinery, 2018, pp. 1–13. Accessed: Sep. 06, 2021. [Online]. Available: https://doi.org/10.1145/3173574.3174075

[96] R. M. Pierce, E. A. Fedalei, and K. J. Kuchenbecker, “A wearable device for controlling a robot gripper with fingertip contact, pressure, vibrotactile, and grip force feedback,” in *2014 IEEE Haptics Symposium (HAPTICS)*, Feb. 2014, pp. 19–25. doi: 10.1109/HAPTICS.2014.6775428.

[97] F. Chinello, M. Malvezzi, C. Pacchierotti, and D. Prattichizzo, “Design and development of a 3RRS wearable fingertip cutaneous device,” in *2015 IEEE International Conference on Advanced Intelligent Mechatronics (AIM)*, Jul. 2015, pp. 293–298. doi: 10.1109/AIM.2015.7222547.

[98] H. Kim, M. Kim, and W. Lee, “HapThimble: A Wearable Haptic Device towards Usable Virtual Touch Screen,” in *Proceedings of the 2016 CHI Conference on Human Factors in Computing Systems*, New York, NY, USA: Association for Computing Machinery, 2016, pp. 3694–3705. Accessed: Sep. 06, 2021. [Online]. Available: https://doi.org/10.1145/2858036.2858196

[99] Y. Yang, Y. Wu, C. Li, X. Yang, and W. Chen, “Flexible Actuators for Soft Robotics,” *Advanced Intelligent Systems*, vol. 2, no. 1, p. 1900077, 2020, doi: 10.1002/aisy.201900077.

[100] J. D. Carrico, T. Tyler, and K. K. Leang, “A comprehensive review of select smart polymeric and gel actuators for soft mechatronics and robotics applications: fundamentals, freeform fabrication, and motion control,” *International Journal of Smart and Nano Materials*, vol. 8, no. 4, pp. 144–213, Oct. 2017, doi: 10.1080/19475411.2018.1438534.

[101] G. M. Whitesides, “Soft Robotics,” *Angewandte Chemie International Edition*, vol. 57, no. 16, pp. 4258–4273, 2018, doi: 10.1002/anie.201800907.

[102] K. Song *et al.*, “Pneumatic actuator and flexible piezoelectric sensor for soft virtual reality glove system,” *Sci Rep*, vol. 9, no. 1, p. 8988, Dec. 2019, doi: 10.1038/s41598-019-45422-6.

[103] G. Frediani and F. Carpi, “Tactile display of softness on fingertip,” *Sci Rep*, vol. 10, no. 1, p. 20491, Dec. 2020, doi: 10.1038/s41598-020-77591-0.

[104] S. S. Robinson *et al.*, “Integrated soft sensors and elastomeric actuators for tactile machines with kinesthetic sense,” *Extreme Mechanics Letters*, vol. 5, pp. 47–53, Dec. 2015, doi: 10.1016/j.eml.2015.09.005.

[105] I. M. Koo, K. Jung, J. C. Koo, J.-D. Nam, Y. K. Lee, and H. R. Choi, “Development of Soft-Actuator-Based Wearable Tactile Display,” *IEEE Transactions on Robotics*, vol. 24, no. 3, pp. 549–558, Jun. 2008, doi: 10.1109/TRO.2008.921561.

[106] A. A. Stanley and A. M. Okamura, “Controllable surface haptics via particle jamming and pneumatics,” *IEEE Trans Haptics*, vol. 8, no. 1, pp. 20–30, Mar. 2015, doi: 10.1109/TOH.2015.2391093.

[107] S. Menon, A. A. Stanley, J. Zhu, A. M. Okamura, and O. Khatib, “Mapping stiffness perception in the brain with an fMRI-compatible particle-jamming haptic interface,” *Annu Int Conf IEEE Eng Med Biol Soc*, vol. 2014, pp. 2051–2056, 2014, doi: 10.1109/EMBC.2014.6944019.

[108] Y.-J. Park, E.-S. Lee, and S.-B. Choi, “A Cylindrical Grip Type of Tactile Device Using Magneto-Responsive Materials Integrated with Surgical Robot Console: Design and Analysis,” *Sensors*, vol. 22, no. 3, Art. no. 3, Jan. 2022, doi: 10.3390/s22031085.

[109] H. Banerjee, M. Suhail, and H. Ren, “Hydrogel Actuators and Sensors for Biomedical Soft Robots: Brief Overview with Impending Challenges,” *Biomimetics*, vol. 3, no. 3, Art. no. 3, Sep. 2018, doi: 10.3390/biomimetics3030015.

[110] P. Won *et al.*, “Transparent Soft Actuators/Sensors and Camouflage Skins for Imperceptible Soft Robotics,” *Advanced Materials*, vol. 33, no. 19, p. 2002397, 2021, doi: 10.1002/adma.202002397.

[111] B. Chen *et al.*, “Stretchable and transparent hydrogels as soft conductors for dielectric elastomer actuators,” *Journal of Polymer Science Part B: Polymer Physics*, vol. 52, no. 16, pp. 1055–1060, 2014, doi: 10.1002/polb.23529.

[112] C. Christianson, N. N. Goldberg, D. D. Deheyn, S. Cai, and M. T. Tolley, “Translucent soft robots driven by frameless fluid electrode dielectric elastomer actuators,” *Sci Robot*, vol. 3, no. 17, p. eaat1893, Apr. 2018, doi: 10.1126/scirobotics.aat1893.

[113] M. Bianchi and A. Serio, "Design and Characterization of a Fabric-Based Softness Display," *IEEE Transactions on Haptics*, vol. 8, no. 2, pp. 152–163, Apr. 2015, doi: 10.1109/TOH.2015.2404353.

[114] Y. Tao, S.-Y. Teng, and P. Lopes, "Altering Perceived Softness of Real Rigid Objects by Restricting Fingerpad Deformation," in *The 34th Annual ACM Symposium on User Interface Software and Technology*, Virtual Event USA, Oct. 2021, pp. 985–996. doi: 10.1145/3472749.3474800.

[115] S. C. Hauser and G. J. Gerling, "Imaging the 3-D deformation of the finger pad when interacting with compliant materials," in *2018 IEEE Haptics Symposium (HAPTICS)*, Mar. 2018, pp. 7–13. doi: 10.1109/HAPTICS.2018.8357145.

[116] S. C. Hauser and G. J. Gerling, "Force-Rate Cues Reduce Object Deformation Necessary to Discriminate Compliances Harder than the Skin," *IEEE Transactions on Haptics*, vol. 11, no. 2, Art. no. 2, Apr. 2018, doi: 10.1109/TOH.2017.2715845.

[117] S. Kim and G. Lee, "Haptic feedback design for a virtual button along force-displacement curves," in *Proceedings of the 26th annual ACM symposium on User interface software and technology*, New York, NY, USA, Oct. 2013, pp. 91–96. doi: 10.1145/2501988.2502041.

[118] H. H. King, R. Donlin, and B. Hannaford, "Perceptual thresholds for single vs. Multi-Finger Haptic interaction," in *2010 IEEE Haptics Symposium*, Mar. 2010, pp. 95–99. doi: 10.1109/HAPTIC.2010.5444670.

[119] B. Li, S. C. Hauser, and G. J. Gerling, "Faster indentation influences skin deformation to reduce tactile discriminability of compliant objects," IEEE Transactions on Haptics, pp. 1–11, 2023